A STUDY OF NEUTRAL B MESON TIME EVOLUTION USING EXCLUSIVELY RECONSTRUCTED SEMILEPTONIC DECAYS

A DISSERTATION
SUBMITTED TO THE DEPARTMENT OF PHYSICS
AND THE COMMITTEE ON GRADUATE STUDIES
OF STANFORD UNIVERSITY
IN PARTIAL FULFILLMENT OF THE REQUIREMENTS
FOR THE DEGREE OF
DOCTOR OF PHILOSOPHY

Timothy Isaac Meyer
August 2002

I certify that I have read this dissertation and that in my opinion it is fully adequate, in scope and quality, as a dissertation for the degree of Doctor of Philosophy.

Patricia Rose Burchat
(Principal Adviser)

I certify that I have read this dissertation and that in my opinion it is fully adequate, in scope and quality, as a dissertation for the degree of Doctor of Philosophy.

Aaron Roodman

I certify that I have read this dissertation and that in my opinion it is fully adequate, in scope and quality, as a dissertation for the degree of Doctor of Philosophy.

Scott Thomas

Approved for the University Committee on Graduate Studies:

Abstract

The Standard Model of particle physics describes the fundamental building blocks of the Universe and their basic interactions. The model naturally describes the time evolution of the basic particles, of which lifetime and mixing are two examples. The neutral B meson, consisting of a bottom quark and an oppositely charged down quark, enjoys a lifetime of about 1.5 ps and the special property of mixing with its antiparticle partner, the $\overline{B}^0$. That is, due to second order weak interactions, the B^0 meson can change into a $\overline{B}^0$ meson and back again as it evolves through time. The details of this behavior offer an opportunity to closely examine the Standard Model.

In this dissertation, I report on a measurement of the lifetime and mixing frequency of the neutral B meson. Using the semileptonic decay channel $B^0 \rightarrow D^{*-}\ell^+\overline{\nu}_\ell$, we select more than 68,000 signal and background candidates from about 23 million $B\overline{B}$ pairs collected in 1999-2000 with the *BABAR* detector located at the Stanford Linear Accelerator Center. The other B in the event is reconstructed inclusively. By constructing a master probability density function that describes the distribution of decay time differences in the sample, we use a maximum likelihood technique to simultaneously extract the B^0 lifetime and mixing parameters with precision comparable to the year 2000 world average. The results are $\tau_{B^0} = (1.523^{+0.024}_{-0.023} \pm 0.022)$ ps and $\Delta m_d = (0.492 \pm 0.018 \pm 0.013)$ ps^{-1}. The statistical correlation coefficient between τ_{B^0} and Δm_d is -0.22.

I describe in detail several cutting-edge strategies this analysis uses to study these phenomena, laying important groundwork for the future. I also discuss several extensions of this work to include possible measurements of higher order parameters such as $\Delta\Gamma_d$.

Foreword

Spokesperson Stewart Smith recently introduced the *BABAR* experiment before the announcement of a new result with the words, "Our experiment has two products: new science, and highly trained people." This is a fundamental statement. I believe the field of physics has two purposes: discoveries about our Universe and the relationships that govern it, and the rigorous training of individuals in the skills of critical thinking, careful observation, and creative vision. This duality is not divisive; rather it is inclusive – it asserts that there is more to the discipline of physics than merely a derived understanding of the Universe. There is a practice, a paradigm, a set of skills that can be developed in physics that has a greater value. It is this dual character that first inspired me to join the field.

This dissertation is about my training in those areas, and it has been an education filled with joy, challenge, and spirit.

FORGET THE WORLD; THE MUSIC IS NOW. - *DJ Zenith*

Acknowledgements

I am grateful for the many gifts in my life. Earning a Ph.D. in Physics at Stanford is no exception, and I will take a moment here to pay my respects before I take the next fork in the road. I am proud of my connection to these people, and shout out my sincere thanks and praise with great enthusiasm.

Pat – As a mentor and advisor she has been a constant source of support and inspiration, embodying the skills of creative vision and mindful observation. As a friend, she's been a model of balance, openness, and sincerity.

David K – Everyone needs a guide when embarking on something unknown, and David has been that older brother, wiser colleague, and the slightly more sober drinking partner. Compassionate, genuine, and dedicated!

Chris and Chih-Hsiang – My drinking buddies, especially when there wasn't even any alcohol around. Brilliant, talented, and good-natured.

Stanford crew – Fil & Nicci, Travis & Taska, John & Danna, Tali & Barbara, Phil & Veronica, Aaron & Kelsey, Gary & Rosemary, Tarek, Aaron & Holly, Pablo & Cathryn, Jason & Heather (& Zoe), and others; all have been the key ingredients in my Bay Area community of family, intimacy, and joy.

The (Extended) Gomez Family – Axis and Allies, "That was a Murali-style hand of cards," and "Arun, you called it on what?!!" I tried to get away by moving to California, but still they found me. And thank goodness they did, for my love and respect for them all has only increased! (Although I'd swear I can still beat them in euchre!)

The Crew at Emilia's – Truly the greatest part of my experience here has been in meeting these friends, and sharing in the quest for understanding what it means to be human and under authority in this life. Especially Tim the Elder, who has been

both father and friend, and who gave me the courage to seek my true intentions.

Tom – Clearly thinking, and thinking clearly. No one could be more honest, understanding, or insightful. A source of unwavering support and confidence, and especially late-night advice. (And thanks to Janis for keeping him around!)

Todd and Jeff – Compadres from a bygone era, these two have always given me the boost I needed to reach the cookie jar on the top shelf.

The Discoverers of Volleyball – Exhilaration, focus, and smacking something really hard. All necessary parts of the happy graduate student existence.

Mom M, Mom & Dad H – A statement on origins: I couldn't have made it here without them. I treasure their encouragement, excitement, and their excellent examples of being; and I thank them for sharing Allison and Emily with me!

BABAR, SLAC – "Crazy" Italians and all, I am indebted to all these wonderful persons' insight, good humor and advice. (Even while on shift!)

Stanford Physics Department – A tremendous environment that nurtured my personal and professional development, and which has always had its heart in the right place.

Emily - My sweetpea, who knew it all was possible. Her deep love for heart, mind, soul, and strength are my inspiration. She's brought unconditional grace, love, and beauty into my life, and her presence has been one of my greatest blessings.

and lastly, Mr. J – he taught me all about Source and Direction.

Finally, if there are some whom I've forgotten or neglected, do write me; the check will be in the mail.

Contents

List of Tables

List of Figures

Chapter 1

Executive Overview

This study examines the time evolution of neutral B *mesons produced at a dedicated collider-detector facility at the Stanford Linear Accelerator Center (SLAC). The collider produces copious amount of* e^+e^- *annihilation events at the* $\Upsilon(4S)$ *resonance. These bound states in turn decay predominantly to* $B\overline{B}$*. Due to the difference in the beam energies in the lab frame, the* B *mesons are boosted in the "forward" direction, and therefore travel about* $250\,\mu\mathrm{m}$ *before decaying. We use the BABAR detector to record the life cycle of the* B *meson.*

Our strategy is to reconstruct candidates in the decay mode $B^0 \rightarrow D^{*-}\ell^+\overline{\nu}_\ell$*, and assign the remaining particle tracks and energy in the event to the other* B *meson decay. By measuring the vertex of each* B*, we estimate the decay distance difference that we convert to the decay time difference* Δt *using our knowledge of the boost between the* $\Upsilon(4S)$ *frame and the lab. We also use charge correlations between the* B *meson decay daughters and the parent candidate to determine the flavor of the constituent* b *quark at the time of decay.*

The quality of the reconstructed $D^*\ell$ *candidate is estimated through a series of fits to the* $m(D^*) - m(D^0)$ *spectrum (after grouping the events into similarly-behaved sub-groups) and by the use of relative efficiencies in similarly selected background control samples. (For instance, a sample of data recorded off the* $\Upsilon(4S)$ *peak is enriched in non-*$B\overline{B}$ *background contributions.) A probability density function for the distribution of all classes of events (signal and backgrounds) is constructed using the control subsamples and taking into account the cross-contaminations, flavor misidentification rates, and decay time difference resolution functions. The 72-parameter model is fit to about* $68,000$ *events from the 1999-2000 BABAR dataset that match our selection criteria. The results include the physics parameters* τ_{B^0} *and* Δm_d*. Consistency checks are performed to validate the technique, and variations of the process are used to estimate the degree of systematic uncertainty.*

The phenomenon of particle-antiparticle oscillations or “mixing” has been observed in neutral mesons containing a down quark and a strange quark (K mesons) or a bottom quark (B mesons) [1], and more recently in the neutrino sector. [2] The time evolution of B^0 mesons is governed by both the overall decay rate $1/\tau_{B^0}$ and the B^0-$\overline{B}^0$ oscillation frequency Δm_d. In the Standard Model of particle physics, this mixing is the result of second-order charged weak interactions involving box diagrams containing virtual quarks with charge 2/3. In B mixing, the diagram containing the top quark dominates. Therefore, the mixing frequency Δm_d is sensitive to the Cabibbo-Kobayashi-Maskawa quark-mixing matrix element V_{td} [3], [4]. In the neutral K meson system, mixing also has contributions from real intermediate states accessible to both a K^0 meson and a $\overline{K}^0$. These contributions are expected to be small for B mixing and are neglected in most of this analysis.

We present a measurement of the B^0 lifetime τ_{B^0} and the oscillation frequency Δm_d based on a sample of approximately 14,000 exclusively reconstructed $B^0 \to D^{*-}\ell^+\overline{\nu}_\ell$ decays selected from a sample of 23 million $B\overline{B}$ events recorded during 1999-2000 at the $\Upsilon(4S)$ resonance with the *BABAR* detector at the Stanford Linear Accelerator Center. In the experiment, 9 GeV electrons and 3.1 GeV positrons annihilate to produce $B\overline{B}$ pairs moving along the electron beam direction (z axis) with a known Lorentz boost of $\beta\gamma = 0.55$, which allows a measurement of the time between the two B decays, Δt.

The proper decay-time difference Δt between two neutral B mesons produced in a coherent P-wave state in an $\Upsilon(4S)$ event is governed by the following probabilities to observe an unmixed event,

$$P(B^0\overline{B}^0 \to B^0\overline{B}^0) \propto e^{-|\Delta t|/\tau_{B^0}}(1 + \cos \Delta m_d \Delta t), \tag{1.1}$$

or a mixed event,

$$P(B^0\overline{B}^0 \to B^0B^0 \text{ or } \overline{B}^0\overline{B}^0) \propto e^{-|\Delta t|/\tau_{B^0}}(1 - \cos \Delta m_d \Delta t). \tag{1.2}$$

Therefore, if we measure Δt and identify the b-quark flavor of each B meson when it decays, we can extract the B^0 lifetime τ_{B^0} and the mixing frequency Δm_d. In this analysis, one B is reconstructed in the mode $B^0 \to D^{*-}\ell^+\overline{\nu}_\ell$, which has a measured branching fraction of $(4.60 \pm 0.21)\%$ [5]. Although the neutrino cannot be detected, the requirement of a reconstructed $D^{*-} \to \overline{D}^0\pi^-$ decay and a high-momentum lepton satisfying kinematic constraints consistent with the decay $B \to D^*\ell\overline{\nu}_\ell$ allows the isolation of a signal sample with (65 - 89)% purity, depending on the D^0 decay mode and whether the lepton candidate is an electron or muon. The charges of the final-state particles are used to identify the meson as a B^0 or a $\overline{B}^0$. The remaining charged particles in the event, which originate from the other B (referred to as B_{tag}), are used to identify, or "tag", its flavor as a B^0 or a $\overline{B}^0$. The time difference $\Delta t = t_{D^*\ell} - t_{\text{tag}} \approx \Delta z/\beta\gamma c$ is determined from the separation Δz along the boost direction of the decay vertices for the $D^*\ell$ candidate and the tagging B. The average separation is $250\,\mu$m.

The oscillation frequency Δm_d and the average lifetime of the neutral B meson, τ_{B^0}, are measured simultaneously with an unbinned maximum-likelihood fit to the measured Δt distributions of events that have been classified as mixed and unmixed. This is in contrast to previous measurements in which only Δm_d is measured with τ_{B^0} fixed to the world average, or in which τ_{B^0} alone is measured. There are several reasons to measure the lifetime and oscillation frequency simultaneously. Since statistical precision for both τ_{B^0} and Δm_d is comparable to the uncertainty on the world average, it is appropriate to measure both quantities rather than fixing the lifetime to the world average. Secondly, since mixed and unmixed events have different Δt distributions, the mixing information for each event improves sensitivity to the Δt resolution function, and a smaller statistical uncertainty on τ_{B^0} results. Also, since $B^0\overline{B}^0$ and B^+B^- events have different mixing behavior, we can use the Δt distributions for mixed and unmixed events to help discriminate between $B^0\overline{B}^0$ signal events and B^+B^- background events in the joint lifetime and mixing measurement.

There are three main experimental complications that affect the Δt distributions given in Eqs. 1.1 and 1.2. First, the tagging algorithm, which classifies events into categories c depending on the source of the available tagging information, incorrectly identifies the flavor of B_{tag} with a probability w_c with a consequent reduction of the observed amplitude for the mixing oscillation by a factor $(1 - 2w_c)$. Second, the resolution for Δt is comparable to the lifetime and must be well understood. The probability density functions (PDF's) for the unmixed (+) and mixed (−) signal events can be expressed as the convolution of the underlying Δt_{true} distribution for tagging category c,

$$\frac{e^{-|\Delta t_{\mathrm{true}}|/\tau_{B^0}}}{4\tau_{B^0}}\,[1 \pm (1-2w_c)\cos\Delta m_d \Delta t_{\mathrm{true}}],$$

with a resolution function $\mathcal{R}(\Delta t_{\mathrm{meas}} - \Delta t_{\mathrm{true}}; \vec{q_c})$ that depends on parameters $\vec{q_c}$. A final complication is that the sample of selected $B^0 \rightarrow D^{*-}\ell^+\overline{\nu}_\ell$ candidates is not pure signal.

This study is described in this document with the following organization. The theoretical framework for B^0 time evolution is presented in Chapter 3, while Chapter 4 discusses other techniques for these measurements and summarizes the current state-of-the-art. An overview of the experimental apparatus is described in Chapter 5. The measurement of Δz and the determination of Δt and $\sigma_{\Delta t}$ for each event is discussed in Chapter 6. The b-quark tagging algorithm is described in Chapter 7. In addition to signal events, control samples of events enhanced in each type of background are selected as described in Chapter 8. Chapter 9 details the general strategy involving fits to the $m(D^*) - m(D^0)$ spectrum and the Δt distributions. The method of determining the signal and background probabilities for each event in the signal and background control samples is discussed in Chapter 10. The physics models and Δt resolution functions used to describe the measured distribution for signal and backgrounds are given in Chapter 11. The likelihood is maximized in a simultaneous fit to the signal and background control samples to extract the B^0 lifetime τ_{B^0}, the mixing frequency Δm_d, the mistag probabilities w_c, the signal Δt resolution parameters $\vec{q_c}$, the background Δt model parameters, and the fraction of $B^\pm \rightarrow D^{*0}\ell^\pm\nu_\ell X$ decays in the signal sample. The results of the fit are given in Chapter 12. Cross-checks are described in Chapter 13 and systematic uncertainties are summarized in Chapter 14. Finally, some future experimental challenges are discussed in Chapter 15.

Chapter 2

Introduction and Motivation

Contemporary understanding of particle physics is encapsulated in the Standard Model, a description of fundamental particles (leptons and quarks) and the relationships between them (mediated by force-carrying bosons). One of these fundamental particles is the b *quark, the second most massive of the six quarks. Although only discovered in 1974 [6], we know a lot about this quark by analogy to its partners, the* s *and* d *quarks and because it has been the subject of intense scrutiny. The Standard Model treats matter and antimatter almost identically (the difference is parameterized by CP violation); so the existence of antimatter is almost unavoidable in this framework. The antiparticle of the* b *quark is the* $\overline{b}$*, which we expect to behave similarly to the* b*. Quarks do not manifest themselves freely in Nature; they are bound into composite particles. The two-quark composite is called a meson, and here we study the* $\overline{B}$ *meson, which contains a* b *quark and a complementary* $\overline{u}$ *or* $\overline{d}$ *quark to make a* B^- *or* $\overline{B}^0$ *meson. The motivation for the study described in this dissertation is to precisely measure the life-cycle of the* B^0 *meson in order to confirm (or reject) the description provided by the Standard Model.*

One prediction of the Standard Model is that B^0 *and* $\overline{B}^0$ *mesons can "mix" or transform into each other and back again according to strict guidelines. Two parameters describing the time evolution (i.e., life-cycle) of the* B^0 *are its lifetime* τ_{B^0} *(how long it lives) and its mixing frequency* Δm_d *(the average rate at which* B^0 *transforms in to* $\overline{B}^0$ *and vice versa). This study uses a novel technique to measure both of these parameters in the same data sample, which consists of a collection of events wherein which we try to identify the "birth" and "death" of each* B *meson, produced at a special facility called PEP-II at the Stanford Linear Accelerator Center. The BABAR experiment is used to record and analyze the* B *meson data, which involves the work of more than 500 scientists. In this study, we seek to identify and characterize a subset of the* B *mesons in the sample by identifying those which decay in a particular way: the semileptonic decay* $B^0 \to D^{*-}\ell^+\overline{\nu}_\ell$*.*

2.1 The Standard Model of Particle Physics

The Standard Model

Current understanding of particle physics is described within the framework of the Standard Model. This picture enumerates the essential sets of particles and describe the forces that act between them. It is under this (somewhat) short list of rules that most of the Universe operates today. However, the Standard Model isn't complete; or rather, it is not yet satisfying as a scientific theory. [*] There are phenomena in Nature that are not described in the Model (such as gravity), and furthermore, we suspect that there are connections between phenomena that we have not yet elucidated. For instance, one needs the physics of Standard Model and 18 parameters [7] in order to cook up the Universe as we presently see it. The 18 independent parameters are divided up between particle masses and strengths of their interactions (couplings); most of these have been determined experimentally (*i.e.,* measured in the lab for our Universe), but not all. Depending on what we learn about the neutrino portion of the Standard Model, we could even see the number of input parameters grow by as much as 9.

The Particles

The Standard Model describes fundamental particles. In general, particles are distinguished from each other by quantum numbers, which are (by construction) those properties of a particle which are conserved under certain interactions. The most familiar quantum numbers include (electric) charge, color, spin, and flavor. Quantum numbers are the key to "telling things apart," and they are used to distinguish individual particles and multi-particle systems (states). Noether's Theorem in quantum field theory [8] guarantees us a conserved quantity for each symmetry of a given system, which can be labelled by the quantum number. Electric charge, for instance, is just the quantum number for a system which corresponds to the conserved quantity associated with a local gauge symmetry. [9].

---

[*] This is an aesthetic impression, perhaps anthropomorphic, but it is widespread.

The basic particles are divided into two groups depending on their spin: *fermions* are those particles who spin is half-integer, and *bosons* are particles with integer spin. The fermion or boson nature of a particle determines what "statistics" it obeys, that is, the rules which must be followed when combining them into multi-particle systems. For instance, fermions obey Fermi statistics, which results in the Pauli Exclusion Principle [10], a statement that no two identical fermions can occupy the same state at the same time. That is, no two identical fermions can have the same quantum numbers. Bosons on the other hand, can occupy the same state, and in fact, multiply occupied states are favored. Fig. 2.1 [11] shows the set of fermions and bosons that are included in the Standard Model.

Matter is made up of the fermions, divided into leptons and quarks, in turn grouped into three families or generations, while all of the force-carrying particles are bosons. Each generation contains one "up-type" quark, one "down-type" quark, a lepton, and a corresponding neutrino. "Up-type" quarks have charge $+2/3$ while "down-type" quarks have charge $-1/3$. Each particle has an antimatter partner that has opposite electric charge and flavor. Quarks can be combined into particles called hadrons, identified as mesons ($q_1\overline{q}_2$) and bayrons ($q_1q_2q_3$).

The meson we study here is the B^0 meson, a $\overline{b}$ quark paired with a d quark. This particle is electrically neutral, and has a corresponding neutral antiparticle, $\overline{B}^0$, composed of a b quark and a $\overline{d}$ quark. Another B meson considered in this analysis is the B^+ meson, which is the charged version, containing instead a u quark partnered with the $\overline{b}$.

The Interactions

The Standard Model describes four fundamental forces in the Universe: gravity, electromagnetism, the weak force, and the strong force (in increasing order of relative strength). Each force is mediated by a set of particles, or rather, represented in particle interactions, by force-carrying bosons. The four forces are depicted in Fig. 2.2 [11].

A key aspect of the Standard Model is the notion of renormalization; this sophisticated notion helps describe how to use the theory once we "place a cut to cancel

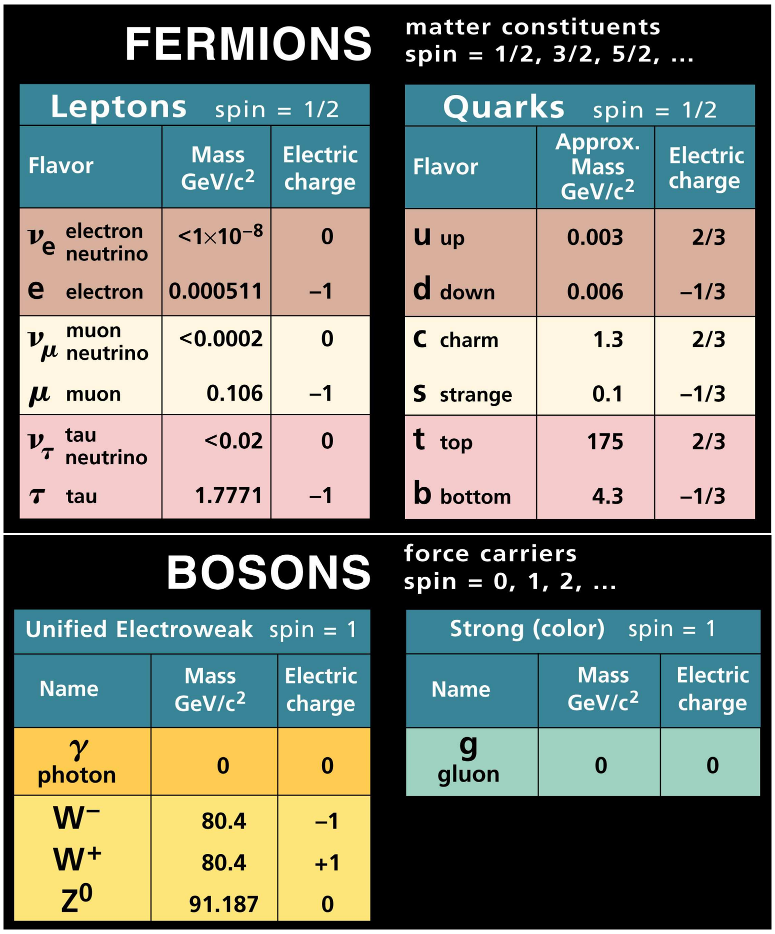

FERMIONS matter constituents
spin = 1/2, 3/2, 5/2, ...

Leptons spin = 1/2

Flavor	Mass GeV/c^2	Electric charge
ν_e electron neutrino	$<1\times10^{-8}$	0
e electron	0.000511	–1
ν_μ muon neutrino	<0.0002	0
μ muon	0.106	–1
ν_τ tau neutrino	<0.02	0
τ tau	1.7771	–1

Quarks spin = 1/2

Flavor	Approx. Mass GeV/c^2	Electric charge
u up	0.003	2/3
d down	0.006	–1/3
c charm	1.3	2/3
s strange	0.1	–1/3
t top	175	2/3
b bottom	4.3	–1/3

BOSONS force carriers
spin = 0, 1, 2, ...

Unified Electroweak spin = 1

Name	Mass GeV/c^2	Electric charge
γ photon	0	0
W^-	80.4	–1
W^+	80.4	+1
Z^0	91.187	0

Strong (color) spin = 1

Name	Mass GeV/c^2	Electric charge
g gluon	0	0

Figure 2.1: Fundamental bosons and fermions defined in the Standard Model of particle physics.

out the infinities" that arise in field theory calculations. But it is actually much more about the observation that the forces can behave differently at different energy scales because we generally work with an *effective* theory. In fact, the Standard Model suggests that unification of the forces is possible at a very high energy scale: although the four forces manifest themselves in an apparently unrelated fashion under ordinary conditions , they can be viewed as different aspects of the same fundamental interaction (at a sufficiently high energy), and so become fundamentally connected at a deep level. One might liken this situation to an ideal gas: at high temperature in the gaseous phase, all of the particles behave identically. As one lowers the temperature, however (*i.e.*, the average energy scale), different substances will begin to liquefy and even solidify before others, taking on very different forms and behaviors. Although this analogy is quite limited, it illustrates one point: in the Standard Model, the four distinct forces (well, except for gravity) we observe now are actually the "frozen-out" components of some higher-energy Grand Unified Force. For instance, we often refer to the combination of the weak and electromagnetic forces above a certain energy threshold (known as the electroweak symmetry breaking scale) as the "electroweak" force.

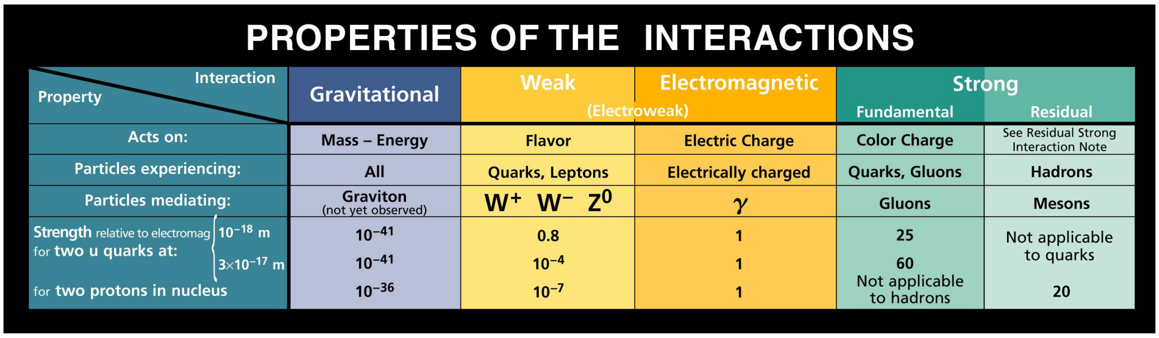

PROPERTIES OF THE INTERACTIONS

Interaction / Property	Gravitational	Weak	Electromagnetic	Strong	
		(Electroweak)		Fundamental	Residual
Acts on:	Mass – Energy	Flavor	Electric Charge	Color Charge	See Residual Strong Interaction Note
Particles experiencing:	All	Quarks, Leptons	Electrically charged	Quarks, Gluons	Hadrons
Particles mediating:	Graviton (not yet observed)	W^+ W^- Z^0	γ	Gluons	Mesons
Strength relative to electromag for two u quarks at: 10^{-18} m	10^{-41}	0.8	1	25	Not applicable to quarks
3×10^{-17} m	10^{-41}	10^{-4}	1	60	
for two protons in nucleus	10^{-36}	10^{-7}	1	Not applicable to hadrons	20

Figure 2.2: Fundamental interactions defined in the Standard Model of particle physics.

The interactions (forces) described by the Standard Model are elegantly summarized in the Standard Model Lagrangian. A Lagrangian is a function that describes the state of a dynamic system in terms of generalized coordinates and their time derivatives. In this study, we are primarily interested in the electroweak portion of the Lagrangrian, because it is responsible for the phenomenon of B^0-$\overline{B}^0$ mixing.

2.1.1 Symmetries

We've already seen several examples of the important role that symmetries play in physics. A particular interaction is often observed to obey many different conservations laws and so the mathematical description of the phenomena has to fulfill stringent invariance requirements. (Conserved quantum numbers are associated with operators that commute with the Hamiltonian.) There are several so-called *discrete* *symmetries* that, if true in the Universe, restrict the class of possible models. These symmetries are C (charge conjugation), P (parity), and T (time reversal).[†] Let us define these symmetries here, as we may revisit some of them in Chapter 15.

Quantum field theory, by construction, seeks to be relativistic, such that the Minkowski interval $t^2 - x^2$ is preserved under transformations both discrete and continuous. The set of continuous transformations that preserve this norm are the Lorentz transformations, including translation, rotations, and boosts. It can be shown that with the addition of three discrete symmetry transformations to the Lorentz group of operators and gauge transformations, one forms a complete basis of the Minkowski interval preserving transformations [13]. These separate transformation can be performed in sequence as well, and one could find that, for instance, while the electroweak interaction violates CP symmetry, it preserves the more general CPT symmetry. CPT has a rather special role in quantum field theory, as it's conservation is guaranteed solely from the reasonable assumptions of Lorentz invariance and locality. [8]

Parity

The *parity* transformation reverses the signs of the 3 spatial components of a four-vector: $(t, x) \to (t, -x)$ and $(E, \vec{p}) \to (E, -\vec{p})$. That is, the effect is to reverse the handedness of a particle, often likened to viewing the particle in a mirror. The effect is to reverse the sign of a particle's momentum while preserving it's spin. The parity operator is unitary, suggested by the property that a second application returns the original state.

Parity was shown to be violated in weak decays in 1957 by Wu *et al.* [14] when examining β decays of ^{60}Co after aligning the cobalt nuclei with an external magnetic field and analyzing the angular distribution of the emitted electron spectrum. This is the classic example of parity violation: the absence of right-handed neutrinos, as

---

[†] One of the primary goals of the *BABAR* experiment is the study of CP-violation in the B^0 meson system. That study is parallel but separate from this analysis, so we choose to avoid that interesting but distracting discussion. See Ref. [12] for more discussion.

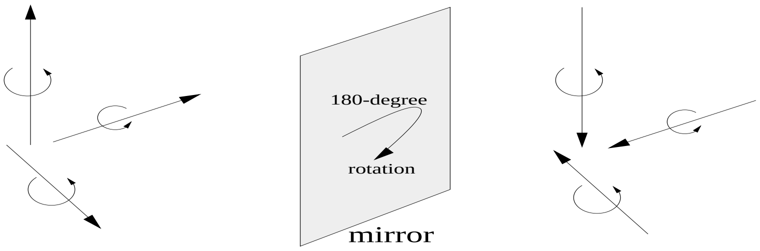

Figure 2.3: Pictorial representation of the parity transformation.

in this decay rate and it's parity-conjugated decay.:

$$\Gamma(\pi^+ \rightarrow \mu^+\nu_L) \neq \Gamma(\pi^+ \rightarrow \mu^+\nu_R) = 0.$$

Charge Conjugation

The charge conjugation transformation is defined to be the transformation of a particle into its antiparticle without changing its momentum or spin (*i.e.,* the particle-antiparticle symmetry operation). Electrodynamics explicitly conserves charge conjugation: although the fields and potentials change their sign under the C symmetry transformation, the Lorentz force incorporates the sign of the charge, and the final physics is invariant. The only eigenstates of the C operator are neutral particles that are their own antiparticle. Charge conjugation symmetry is violated in weak decays, as indicated in this pair of decay rates (there are no left-handed anti-neutrinos):

$$\Gamma(\pi^+ \rightarrow \mu^+\nu_L) \neq \Gamma(\pi^- \rightarrow \mu^-\overline{\nu}_L) = 0.$$

Time Reversal

The time reversal transformation reverses the momentum and spin of a particle and reverses the sign of the time component (*i.e.,* interchanging the forward and backward light-cones). This is often likened to watching a film of the process in reverse. If the CPT theorem is true for our Universe, we expect to see time reversal violation in weak decays, since we've already seen that CP is not conserved. Because the experiments are challenging, evidence for time reversal violation has only recently observed by CPLEAR. [‡] [15]

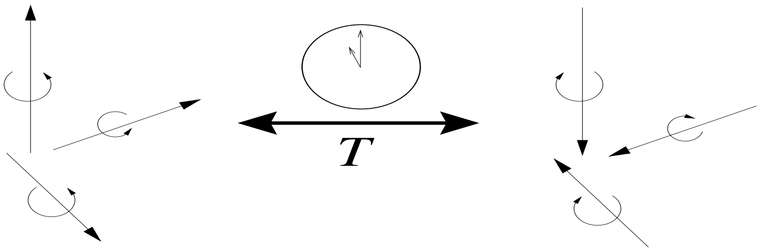

Figure 2.4: Pictorial representation of the time-reversal transformation.

	C	P	T	CP	CPT
Scalar	+1	+1	+1	+1	+1
Pseudoscalar	+1	-1	-1	-1	+1
Vector	-1	$\begin{pmatrix} +1 \\ -1 \\ -1 \\ -1 \end{pmatrix}$	$\begin{pmatrix} +1 \\ -1 \\ -1 \\ -1 \end{pmatrix}$	$\begin{pmatrix} -1 \\ +1 \\ +1 \\ +1 \end{pmatrix}$	-1
Pseudovector	+1	$\begin{pmatrix} -1 \\ +1 \\ +1 \\ +1 \end{pmatrix}$	$\begin{pmatrix} +1 \\ -1 \\ -1 \\ -1 \end{pmatrix}$	$\begin{pmatrix} -1 \\ +1 \\ +1 \\ +1 \end{pmatrix}$	-1
Tensor	-1	$\begin{pmatrix} +1 & -1 & -1 & -1 \\ -1 & +1 & +1 & +1 \\ -1 & +1 & +1 & +1 \\ -1 & +1 & +1 & +1 \end{pmatrix}$	$\begin{pmatrix} -1 & +1 & +1 & +1 \\ +1 & -1 & -1 & -1 \\ +1 & -1 & -1 & -1 \\ +1 & -1 & -1 & -1 \end{pmatrix}$	$\begin{pmatrix} -1 & +1 & +1 & +1 \\ +1 & -1 & -1 & -1 \\ +1 & -1 & -1 & -1 \\ +1 & -1 & -1 & -1 \end{pmatrix}$	+1
Derivative Operator	+1	$\begin{pmatrix} +1 \\ -1 \\ -1 \\ -1 \end{pmatrix}$	$\begin{pmatrix} -1 \\ +1 \\ +1 \\ +1 \end{pmatrix}$	$\begin{pmatrix} +1 \\ -1 \\ -1 \\ -1 \end{pmatrix}$	-1

Table 2.1: Table of how the discrete symmetry operators, C, P, and T affect the basic Lorentz objects: eigenvalues and transformed objects are shown as appropriate.

[‡] Indeed, one prospect for *BaBar* is the observation of time reversal violation in b quark system.

2.1.2 Comments on the Electroweak Interaction

The electroweak Lagrangian is based on the SU(2)×U(1) symmetry group containing four bosons: a massless isovector triplet $\mathbf{W}_\mu$ for the SU(2) of weak isospin, and a massless isosinglet B_μ for the the U(1) of weak hypercharge. [16] Above the spontaneous symmetry-breaking threshold, all four bosons ($W^\pm, W^0, B^0$) are massless and the SU(2)×U(1) symmetry is unbroken. Below the symmetry-breaking threshold, the charged bosons and one linear combination of the neutral bosons acquire mass ($W^\pm, Z^0$) while the orthogonal combination of neutral bosons remains massless (the photon). The SU(2)×U(1) symmetry is thus not completely broken. There remains a U(1) symmetry which gives rise to electromagnetism and the photon.

Following the discussion in Ref. [17], we can write out the interaction term in explicit form:

$$\mathcal{L}_{\mathrm{EW}} = -i\left[g\mathbf{J}^\mu \cdot \mathbf{W}_\mu + \frac{g'}{2}(J^Y)^\mu B_\mu\right]. \tag{2.1}$$

This is elegant and compact, but requires some explanation. Loosely speaking, we define the components as

- $\mathbf{W}_\mu$ is the isotriplet of massless Yang-Mills gauge fields (bosons) introduced to preserve the SU(2) symmetry of the Lagrangian,

- B_μ is the isosinglet gauge field associated with the U(1) symmetry for weak hypercharge Y,

- $\mathbf{J}^\mu$ is the weak isopin current, *i.e.,* a combination of fermions fields[§] that is conserved due to the SU(2) symmetry of weak isospin [¶] (in fact, this symmetry is only applied to left-handed fermion fields),

- J^Y is the weak hypercharge current, *i.e.,* a combination of fermion fields that is conserved due to the U(1) symmetry (operating on both left- and right-handed fermion fields),

---

[§] In fact, if we impose Lorentz invariance upon our Lagrangian, we are restricted to a finite set of ways in which we can combine fermion fields to form these currents!

[¶] There are *three* conserved charges, corresponding to the three isospin components of $\mathbf{J}^\mu$.

- g is the coupling of the isotriplet of vector fields $\mathbf{W}_\mu$ to the weak isospin current $\mathbf{J}^\mu$,

- $\frac{g\prime}{2}$ is the coupling of the vector field B_μ to the weak hypercharge current, J^Y

This model assumes all the particles (both the fermions and bosons) are massless. To observe the unification of electromagnetism and the weak interaction, we note that the fields W^3_μ and B_μ are neutral fields, and can be linearly combined (*mixed*) to form the physical fields A_μ and Z_μ:

$$\begin{aligned} W^\pm_\mu &= \frac{1}{\sqrt{2}}(W^1_\mu \mp iW^2_\mu) \\ A_\mu &= B_\mu \cos\theta_W + W^3_\mu \sin\theta_W \\ Z_\mu &= -B_\mu \sin\theta_W + W^3_\mu \cos\theta_W. \end{aligned} \tag{2.2}$$

Identifying $g/g\prime = \tan\theta_W$ and substituting back into the Lagrangian term with $J^\pm_\mu \equiv J^1_\mu \pm J^2_\mu$, we arrive at:

$$\mathcal{L} = \frac{g}{\sqrt{2}}(J^-_\mu W^+_\mu + J^+_\mu W^-_\mu) + \frac{g}{\cos\theta_W}(J^3_\mu - \sin^2\theta_W J^{e.m.}_\mu)Z_\mu + g\sin\theta_W J^{e.m.}_\mu A_\mu, \tag{2.3}$$

where the first term can be associated with the weak charged current interaction, the second with the weak neutral current, and the final one with the traditional electromagnetic neutral current. To make the identification complete, we assign $e = g\sin\theta_W = g'\cos\theta_W$, where θ_W is called the weak mixing (or Weinberg) angle. [18] The neutral fields Z_μ and A_μ are distinct operators and correspond to the Z^0 and photon particles with definite mass, and the charged $W^\pm_\mu$ fields correspond to the charged $W^\pm$ bosons.

We summarize our discussion of the unbroken electroweak theory by showing the interaction between the gauge bosons and the fermions. First, we explicitly write out the fermionic field components of the conserved currents: (here for leptons)

$$\begin{aligned} J_\mu^- &= \overline{\nu}_L \gamma_\mu e_L \\ J_\mu^+ &= \overline{e}_L \gamma_\mu \nu_L \\ J_\mu^3 &= \frac{1}{2}\overline{\nu}_L \gamma_\mu \nu_L - \frac{1}{2}\overline{e}_L \gamma_\mu e_L \\ J_\mu^Y &= -2\overline{e}_R \gamma_\mu e_R - \overline{e}_L \gamma_\mu e_L - \overline{\nu}_L \gamma_\mu \nu_L \end{aligned} \tag{2.4}$$

We can then generalize to include quarks and write for the general Dirac spinor ψ,

$$\begin{aligned} J_\mu^\pm &= \sqrt{2}\overline{\psi}\gamma_\mu \mathbf{T}^\pm \psi \\ Z_\mu &= \overline{\psi}\gamma_\mu [T_3 - \sin^2\theta_W Q]\psi \\ J_\mu^{e.m.} &= \overline{\psi}\gamma_\mu Q \psi \end{aligned} \tag{2.5}$$

where $\mathbf{T}$ is the weak isospin operator (vanishing on ψ_R and having representation $\mathbf{T} = \frac{1}{2}\tau$ with the Pauli matrices τ for the isodoublets ψ_L), and Q is the electric charge. All the fermion fields, now, can interact with the gauge fields.

The gauge bosons are still massless in this description, however (as are the fermions). We accommodate massive gauge bosons by introducing the *Higgs field* Φ, an SU(2) doublet of scalar fields. We arrange for the potential to have a ground state with non-vanishing expectation value in the physical vacuum state. Spontaneously breaking this symmetry generates masses while maintaining renormalizibility, but leaves the gauge symmetry of the Lagrangian hidden; we have introduced a preferred direction in weak isospin-hypercharge space. Without going into details, the procedure is to add a potential to the Lagrangian for the new Higgs field:

$$V = \mu^2|\Phi|^2 + \lambda|\Phi|^4 \qquad \mathcal{L}_\Phi = |D_\mu\Phi|^2 - V(|\Phi|^2)\ , \tag{2.6}$$

where we have introduced the new weak isodoublet of fields

$$\Phi = \begin{pmatrix} \Phi^+ \\ \Phi^0 \end{pmatrix}\ . \tag{2.7}$$

We require $\lambda > 0$ to bound the potential as $\Phi \to \infty$, and consider the "interesting" case where $\mu^2 < 0$. The potential V has a minimum along $\Phi^\dagger\Phi = -\frac{\mu^2}{2\lambda}$, a locus of points that is invariant under rotations in the SU(2) space. We study the particle spectrum, which requires perturbation theory near the minimum. We must choose a particular direction in which to expand, however. This spontaneously breaks the SU(2) symmetry.

The original field Φ had four degrees of freedom, one for each Φ_i. The Standard Model choice for Φ is $\Phi_1 = \Phi_2 = \Phi_4 = 0, \Phi_3^2 \equiv v^2$, bringing us to

$$\Phi(x) = \frac{1}{\sqrt{2}} \begin{pmatrix} 0 \\ v + h(x) \end{pmatrix} . \tag{2.8}$$

We have eliminated three degrees of freedom by choosing the *unitary* gauge such that three of the four fields have been absorbed. This is "legal" since the Lagrangian is symmetric under local gauge transformations. However, these three degrees of freedom will later emerge as mass terms for the gauge fields themselves.

The requirement of local gauge symmetry requires the introduction of a massless vector field and associated covariant derivatives, and so with the addition of Φ, we modify the Lagrangian appropriately. We obtain Higgs-$\mathbf{W}_\mu$ and Higgs-B_μ interactions from the covariant derivative, after substituting in the form of Φ as chosen above:

$$|D_\mu\Phi|^2 \sim |(-ig\frac{\tau}{2} \cdot \mathbf{W}_\mu - i\frac{g'}{2}B_\mu)\Phi|^2 \tag{2.9}$$

$$= \frac{1}{8} \left| \begin{pmatrix} gW_\mu^3 + g'B_\mu & g(W_\mu^1 - iW_\mu^2 \\ g(W_\mu^1 + iW_\mu^2 & -gW_\mu^3 + g'B_\mu \end{pmatrix} \begin{pmatrix} 0 \\ v \end{pmatrix} \right|^2 . \tag{2.10}$$

Working through the math and using the mixed fields A_μ and Z_μ that we already deduced in the electroweak unification, we arrive at the conclusions for the masses of the photon, Z^0, and $W^\pm$:

$$m_A = 0 \tag{2.11}$$

$$m_Z = \frac{1}{2}\sqrt{g^2 + g'^2} \tag{2.12}$$

$$m_W = \frac{1}{2}vg \tag{2.13}$$

$$m_h = \sqrt{-2\mu^2} \tag{2.14}$$

The physical states with mass are the full set of final bosons: the charged particles, $W^\pm$, and the neutrals Z^0 and A_μ (the photon), and of course, the Higgs. The result of the Higgs mechanism is that vacuum everywhere can emit or absorb (colorless) quanta of the Higgs field that carry weak isospin and hypercharge. The fermions, W, and Z bosons which can couple to the quantum field effectively gain mass, but particles such as the photon and gluon which do not interact with it remain massless. In summary, the Lagrangian has remained gauge invariant, but the vacuum has not.

2.1.3 The CKM Matrix

Fermion masses can be generated in the spontaneous symmetry breaking mechanism if we include Yukawa interactions between the physical states and Higgs field Φ (using coupling parameters g and the conjugate isodoublet $\tilde{\Phi}$) of the form

$$g_d^{ij}(\overline{u}_i, \overline{d}_i)_L \tilde{\Phi}^\dagger d_{j_R} + g_u^{ij}(\overline{u}_i, \overline{d}_i)_L \Phi^\dagger u_{j_R} + h.c. \;, \tag{2.15}$$

where we have just used the quark doublets $(u_i, d_i)_L$ and $i, j = \{1..3\}$ corresponding to the three generations. However, the weak interactions actually operate on the isospin doublets, $(u_i, d'_i)_L$, which is, in general, a different set of basis vectors. We are forced to introduce the unitary mixing matrix V, the so-called CKM matrix [4] which rotates the quark mass eigenstates into the weak eigenstates. (In short, the mass eigenstates are not weak eigenstates.)

$$\begin{pmatrix} d' \\ s' \\ b' \end{pmatrix} = \begin{pmatrix} V_{ud} & V_{us} & V_{ub} \\ V_{cd} & V_{cs} & V_{cb} \\ V_{td} & V_{ts} & V_{tb} \end{pmatrix} \begin{pmatrix} d \\ s \\ b \end{pmatrix} \tag{2.16}$$

The modified form of the charged current, for instance, is

$$J^{+}_{L\mu} = \overline{(u,c,t)}_L \gamma_\mu \mathsf{V} \begin{pmatrix} d \\ s \\ b \end{pmatrix}_L . \tag{2.17}$$

Note that this mixing occurs only in the quark sector since we have assumed that the neutrinos are massless; such mixing is therefore "invisible" in the lepton sector. By convention, the mixing is assigned completely to the "down-type" quarks.

The CKM matrix V is a complex, unitary matrix. As such, it has at most 9 independent real parameters since the unitarity conditions offer 9 constraints on the original set of 18 parameters.

$$\mathsf{V}^\dagger \mathsf{V} = \mathsf{V}\mathsf{V}^\dagger = \mathit{1} \quad \Rightarrow \quad \sum_j \mathsf{V}^*_{ji} \mathsf{V}_{jk} = \sum_j \mathsf{V}_{ij} \mathsf{V}^*_{kj} = \delta_{ik} \tag{2.18}$$

Furthermore, we can absorb a relative phase in each left-handed field, eliminating 5 more degrees of freedom. This leaves us with 4 physically independent parameters describing the CKM matrix [‖], and as such, can be envisioned as three Euler angle rotations and one phase insertion. [**]

The charged current portion of the electroweak Lagrangian for the quark fields

---

[‖] In general, the CKM matrix for N generations has $(N-1)^2$ parameters.

[**] Recall that the general $N \times N$ unitary matrix has N^2 independent parameters. The fundamental representation of SO(N) uses $N \times N$ orthogonal matrices which have $(N^2 - N)/2$ independent parameters, where each matrix represents a rotation around a real axis. Finally, we compare the number of free parameters in the CKM matrix to the number of the SO(N) matrix: $(N-1)^2 - (N^2 - N)/2 = \frac{1}{2}(N-1)(N-2)$. This difference is the excess of parameters which cannot be associated with rotations about any of N available axes. $N > 2$ is required to have a positive excess, and hence to enjoy CP violation in the CKM matrix.

becomes

$$\mathcal{L}^{cc}_{\rm EW} = \frac{g}{\sqrt{2}} \left\{ \bar{u}^L_i \gamma^\mu W^+_\mu V_{ij} d^L_j + \bar{d}^L_i \gamma^\mu W^-_\mu V^*_{ij} u^L_j \right\} \tag{2.19}$$

with u^L_i representing the vector of up-type quarks and d^L_i representing the down-type quarks. Applying the *CP* operator to the Lagrangian, one obtains:

$$CP(\mathcal{L}^{cc}_{\rm EW}) = \frac{g}{\sqrt{2}} \left\{ \bar{d}^L_i \gamma^\mu W^-_\mu V_{ij} u^L_j + \bar{u}^L_i \gamma^\mu W^+_\mu V^*_{ij} d^L_j \right\} \tag{2.20}$$

which is identical to Eq. 2.19 for the complex conjugation of V if we reverse of order of the summands. Thus, if we could find a basis for which the elements of V are real, then *CP* is a good symmetry. Based on our parameter counting earlier, we saw that in general, the CKM matrix will have a complex phase, which would generate *CP* violation as described here if we can show it to be non-zero.

The unitarity conditions on the CKM matrix are often used to construct so-called "triangles" in the complex plane. We list the six vanishing ones here for completeness (the diagonal products yield unity):

$$V_{cd}V^*_{ud} + V_{cs}V^*_{us} + V_{cb}V^*_{ub} = 0 \tag{2.21}$$

$$V_{cd}V^*_{td} + V_{cs}V^*_{ts} + V_{cb}V^*_{tb} = 0 \tag{2.22}$$

$$V_{ud}V^*_{td} + V_{us}V^*_{ts} + V_{ub}V^*_{tb} = 0 \tag{2.23}$$

$$V^*_{us}V_{ud} + V^*_{cs}V_{cd} + V^*_{ts}V_{td} = 0 \tag{2.24}$$

$$V^*_{ub}V_{us} + V^*_{cb}V_{cs} + V^*_{tb}V_{ts} = 0 \tag{2.25}$$

$$V^*_{ub}V_{ud} + V^*_{cb}V_{cd} + V^*_{tb}V_{td} = 0 \tag{2.26}$$

The last unitarity condition listed is traditionally the one used to construct the "Unitarity Triangle," a geometrical way of depicting the vanishing sum of three complex numbers; see Fig. 2.5.

The relative sizes of the CKM elements are key to understanding electroweak interaction rates. The most popular parameterization uses four values (λ, A, ρ, η) to

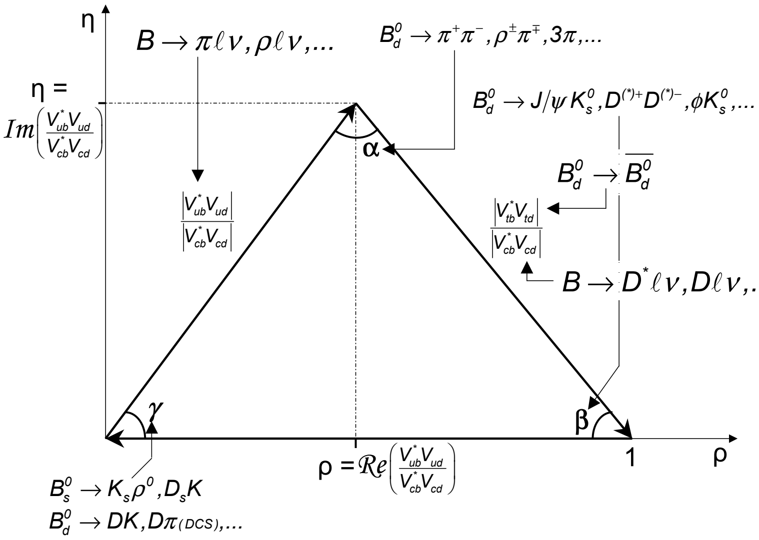

Figure 2.5: The standard CKM triangle expresses the unitarity condition between the first and third columns.

describe the matrix in the following way (known as the Wolfenstein parameterization [19]):

$$V_{CKM} = \begin{pmatrix} 1 - \frac{1}{2}\lambda^2 & \lambda & A\lambda^3(\rho - i\eta) \\ -\lambda & 1 - \frac{1}{2}\lambda^2 & A\lambda^2 \\ A\lambda^3(1 - \rho - i\eta) & -A\lambda^2 & 1 \end{pmatrix} + \mathcal{O}(\lambda^4). \tag{2.27}$$

We observe that the diagonal elements are indeed the largest, and furthermore that some of the entries are very small (the ranges are the experimental bounds):

$$|V_{CKM}^{ij}| = \begin{pmatrix} 0.9742 - 0.9757 & 0.219 - 0.226 & 0.002 - 0.005 \\ 0.219 - 0.225 & 0.9734 - 0.9749 & 0.037 - 0.043 \\ 0.004 - 0.014 & 0.035 - 0.043 & 0.9990 - 0.9993 \end{pmatrix}. \tag{2.28}$$

Perspective

Where has this taken us? We have described the weak component of the Standard Model Lagrangian, and as such we have understood that it can be responsible for flavor-changing charged current interactions. And because of the $\mathrm{SU}(2)_L$ symmetry of weak isospin, the "down-type" quarks can mix according to the charged current prescription. In particular, we see that the the b quark can change flavor to a c quark via a charged current interaction. Later we'll see that it is possible for a b quark to transition into a d quark, via second order processes (*i.e.,* loops). Finally, we've seen two examples of the idea of "mixing": the mass eigenstates of the quarks are mixed to form the weak eigenstates, and the two neutral components of the electoweak gauge field were mixed to form the neutral and electromagnetic currents. The lesson is that if there's more than one interaction in a theory, the natural basis for one interaction will not necessarily be the states distinguished by another, *i.e.,* different dynamical processes usually have distinct sets of eigenstates that will be linear combinations of each other.

2.1.4 Lifetime

We next give meaning to the lifetime of a particle, since the measurement of the lifetime of the B^0 meson is one of the two goals of this study. By lifetime, we refer to the length of time between the "birth" and "decay" of a particle. The decay of any particular particle is a random process, but in an ensemble of many particles we can describe the average evolution by observing that the ensemble population decreases at a constant fractional rate. The decay process is stochastic or "memoryless," which means that the chance of decay for a particle is independent of how long it has "lived" so far. These observations lead to the following mathematical description. Introducing the decay rate Γ, we write the differential equation relating the fractional decay rate to the population at time t:

$$\frac{dN}{dt} = -\Gamma \cdot N(t) \tag{2.29}$$

$$\therefore N(t) = N(0) \exp^{-\Gamma t} \ . \tag{2.30}$$

The solution is the familiar negative exponential, and we define the lifetime $\tau \equiv 1/\Gamma$ to be the time that it takes for $(1 - 1/e) \sim 64\%$ of the population to decay. We call Γ

the decay rate in general, and in particle physics in particular, we also call it the *decay width*. At any point in time, a surviving particle has a $1/e$ chance of surviving for another lifetime. Again, the lifetime for any particular particle is a random variable, but in an ensemble we observe that the distribution of many particles' lifetimes follows a negative exponential law.

Most composite particles decay quickly. It is only in "rare" circumstances where special symmetries are at work that composite particles have an extended lifetime. Particles can decay via the strong, weak or electromagnetic forces, which operate on characteristically different timescales. Typical lifetimes are generally determined by the force mediating the decay, but the kinematics of the decay and various symmetries can also greatly affect the result. The typical lifetime for particles decaying strongly is 10^{-23} sec, electromagnetically 10^{-16} sec, and decaying weakly is about 10^{-8} sec.

The decay of any particle can be factorized into two parts: one part representing the pure kinematics of the decay (the so-called *phase space* contribution) and the other part the matrix element between the initial and final states. Note that the heavier mesons will have larger phase space available for decays, making them generally shorter-lived. The matrix element carries the information about the physics involved in the particular decay.

For the decay $X \to 1 + 2 + ... + n$: [9], the differential decay rate is

$$d\Gamma = \frac{1}{2E_X}|\mathcal{M}|^2 \frac{d^3p_1}{(2\pi)^3 2E_1} ... \frac{d^3p_n}{(2\pi)^3 2E_n}(2\pi)^4\delta^{(4)}(p_X - p_1 - ... - p_n) \qquad (2.31)$$

where $\mathcal{M} = \langle f|\mathcal{H}|i\rangle$ is the matrix element sandwich about the interaction Hamiltonian, $\mathcal{H}$. The matrix element represents the overlap between the initial and final states, as described by the physics at work, and is really a measure of the connection between them. Angular dependence can be delivered by the matrix element $\mathcal{M}$, amongst other differential properties, which is why we write Eq. 2.31 as the differential decay rate. The net decay width to a specific final state i, after integrating over all differentials is the partial decay width Γ_i. The total decay rate of a particle is the sum of all individual channels:

$$\Gamma_{total} = \sum \Gamma_i \ . \tag{2.32}$$

This in turn means that the lifetime of a particle is determined by the details of all its available decay channels, both in number and in kind. This is a powerful statement: we cannot speak of the "lifetime for the decay to a particular final state'," although the partial decay widths control the overall lifetime. [*] For instance, the difference in lifetimes for the B^0-$\overline{B}^0$ system is controlled by the difference in available number of decay modes. We'll learn more about the B^0 lifetime, τ_{B^0}, in Chapter 3.2.

2.1.5 Mixing

We now introduce the second parameter which this analysis measures, the mixing frequency of the B^0-$\overline{B}^0$ meson system, Δm_d. We've already seen some examples of mixing when we discussed the electroweak sector of the Standard Model. The key idea is that mixing occurs because the flavor eigenstates are not equivalent to the mass eigenstates; *i.e.,* one cannot measure both the mass and the flavor of the particle simultaneously. As such, time evolution (according to the Hamiltonian governing the system) will rotate the flavor eigenstates as a function of time while it preserves the mass eigenstates. In the Standard Model, the four pairs of neutral mesons that decay weakly share the mixing diagrams shown in Fig. 2.1.5. Such a process is the result of second-order charged current interactions involving box diagrams containing virtual quarks.

The details of the mixing, of course, depend on the meson pair under consideration. Because of the different CKM matrix elements in question (as mentioned before, these mixing diagrams rely on the charged current interaction), mixing occurs at different rates in each of the neutral meson conjugate pair systems. For instance, K^0-$\overline{K}^0$ mixing relies on the CKM matrix elements $V_{is} \times V_{id}$ which is of order λ, but the matrix elements of the B^0-$\overline{B}^0$ system are instead of $\mathcal{O}(\lambda^3)$ and significantly suppressed.

---

[*] Quantum mechanics is also at work here: we don't know how the particle will decay until we actually see that it does.

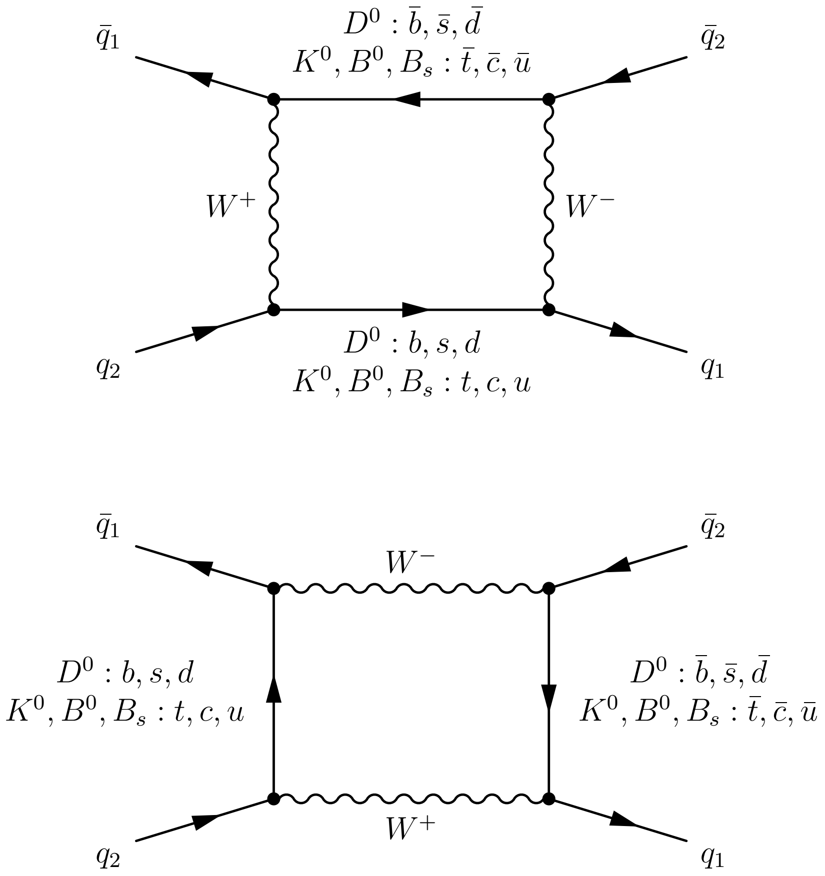

Figure 2.6: The two mixing diagrams for K^0-$\overline{K}^0$, D^0-$\overline{D}^0$, B^0-$\overline{B}^0$ and B_s-$\overline{B}_s$ neutral mesons systems. The upper Feynman graph depicts the W-exchange diagram, the lower one the box diagram. At each vertex, we accumulate a factor of the corresponding CKM matrix element.

The mass eigenstates of the full Hamiltonian are linear combinations of the flavor eigenstates. Let X^0 and $\overline{X}^0$ be the so-called flavor eigenstates of definite quark content that are most useful in understanding particle production and decay, and let X_H and X_L be the states of definite mass and lifetime which propagate through space in a definite fashion. We then write the general superposition as:

$$\begin{aligned} |X_H\rangle &= p_H|X^0\rangle - q_H|\overline{X}^0\rangle \\ |X_L\rangle &= p_L|X^0\rangle + q_L|\overline{X}^0\rangle. \end{aligned} \tag{2.33}$$

The two states X_H and X_L have different time evolution, so the flavor of the state evolves in time as well. The mass splitting Δm of X_H and X_L is dominated by virtual (off-shell) transitions while real intermediate states (*i.e.,* the imaginary parts of the box diagram, here via real c and u quarks) contribute to the lifetime difference $\Delta\Gamma$. † In general, virtual transitions are suppressed by the GIM mechanism [9], but these cancellations aren't perfect due to differences in the various quark masses. In the B^0 mixing system, for instance, the relevant products of CKM matrix elements are of the same order, and the mass hierarchy of the quarks comes into play, making the t quark dominant. In the K^0 system, however, the t quark transitions are suppressed, leaving the c quark dominant.

In preparation for later discussions, let us note that:

- *CPT* invariance would require that $p_H = p_L$ and $q_H = q_L$
- *T* invariance would require that $|q_L/p_L| = 1$ and $|q_H/p_L| = 1$
- *CP* invariance (in mixing) would require $p_L = p_H = p$, $q_L = q_H = q$, and that $|p/q| = 1$.

We'll discuss the structure of the time evolution more formally in Chapter 3. From the present discussion, however, we can already see that the time dependence of the system will depend on both Δm and $\Delta\Gamma$. We call Δm the mixing frequency when it dominates. A useful figure-of-merit in this scenario is the ratio of the mixing frequency to the average lifetime, which describes "how many times the meson can mix before it decays." For the B^0 system, $\frac{\Delta m}{\Gamma} \sim 0.7$, while for the B_s system, $\frac{\Delta m}{\Gamma} \sim 14.0$. In the K^0 system, the lifetime difference is large, but the equivalent figure of merit might be the mass splitting divided by the shorter K^0_S lifetime component, yielding $\frac{\Delta m}{\Gamma} \sim 0.6$. (These values have not yet been established for the D^0 system.)

For these neutral mesons, a difference in lifetimes between the elements of the pair can only arise from decay channels in common to both mesons. The best way to think about this is in the case of *CP* conservation ($|p| = |q|$): only when the final

---

[†] Recall from ordinary quantum mechanics that degenerate states will undergo "splitting" when an interaction Hamiltonia is introduced that couples them.

state f is accessible to X^0 and $\overline{X}^0$ (*i.e.,* a *CP* eigenstate perhaps) will the different admixture of X and $\overline{X}^0$ in X_H and X_L become apparent and the partial widths to f will be different. [‡] For the heavier mesons, the lifetime difference is expected to be smaller than the average lifetime since the branching ratios to the states accessible to both of the pair is small, and therefore the "opportunity" for final states in common is reduced. CKM factors come can come into play, however, to create additional suppression. For instance, when comparing the expected width difference $\Delta\Gamma$ in the B_s and B_d systems, note that such decays would involve $b \to c\bar{c}q$ where $q = d$ or s. These decays are Cabibbo-suppressed if $q = d$ and Cabibbo-allowed if $q = s$; we therefore expect $\Delta\Gamma/\Gamma$ to be as much as 20% in the B_s system, but less than 1% ($\lambda^2\Delta\Gamma_s/\Gamma_s$) in the B^0 system.

2.2 Goals of this Study

The goal of this study is to understand the life cycle of the B meson by measuring the parameters Δm_d and τ_{B^0} with high precision. In doing so, we will pioneer the technique for measuring these parameters simultaneously, and will establish a deep level of understanding of so-called "time dependent analyses" that will be critical for many other measurements at *BABAR* and elsewhere.[§]

We motivate our study of B^0-$\overline{B}^0$ lifetime by observing that the interesting part of a particle's decay rate comes from the contribution from the matrix element (see Eq. 2.31) since this piece encapsulates the complex physics. There is much interest in this term because the b quark is so much heavier than the d (and u and s) quark that the phenomenologist typically assumes that the light quark's flavor doesn't matter. The approximation that the dynamics of the meson are dominated by the heavy quark is called the *spectator* model. [20] Empirically however, we know this model isn't very accurate in the D system. By studying the B^0 lifetime, we seek to improve

---

[‡] If *CP* violation occurred, $\Delta\Gamma$ might even be exacerbated because, for example, both B^0 and $\overline{B}^0$ can decay to D^+ D^-, but if the particular rate for $B^0 \to D^+D^-$ were to be greater than $\overline{B}^0 \to D^+D^-$, (*CP* violating) the B^0 would decay more quickly due to the larger partial width.

[§] Other time-dependent analyses include those measuring the CKM angles sin2β, sin2α, and sin2γ (see Fig. 2.5).

our understanding of the relationship between the light companion quark and the much heavier b quark.

Our study of the B^0 mixing frequency is motivated by two goals: (1) the loops in the box diagrams may be sensitive to the introduction of new physics, and (2) because Δm_d depends on V_{td}, a relatively poorly measured element of the CKM matrix, we can improve our estimate of V_{td}. By precisely comparing the measured value of Δm_d with that predicted by the Standard Model, we can, with a certain degree of confidence, exclude the presence of new physics in the loop processes.

We are also interested in B^0-$\overline{B}^0$ time evolution from a larger perspective. Because the system includes neutral meson mixing and decay, it is an excellent environment for testing the symmetries of the Standard Model.

2.3 Methods of this Study

Exploring the B system and its potential impact on the Standard Model requires copious production of B mesons, accurate measurement of the B flight path and flavor, and reasonably low backgrounds for reconstruction. This section introduces the key experimental principle used to achieve this. Note that we use the term *flavor* to label the flavor of the b quark within the B meson.

2.3.1 Collisions at the $\Upsilon(4S)$

In e^+e^- interactions, there is a resonant state $\Upsilon(4S)$ near $E_{cm} = 10.58\,\mathrm{GeV}$ that decays almost exclusively to b-$\overline{b}$ pairs. As the b quarks hadronize, lighter quarks are pulled from the vacuum, creating two B mesons that separate. Depending on the flavor of the spontaneously generated light quarks, the B mesons are either charged or neutral. By isospin symmetries, this implies 50% B^+B^- and 50% $B^0\overline{B}^0$ pairs. The $\overline{b}$ production cross-section near the $\Upsilon(4S)$ peak (see Fig. 2.7) is about 1 nb, which is about one-third as much as other continuum processes, and comparable to the $\mu^+\mu^-$, $\tau^+\tau^-$ pair production rates as well. The dominant physics, of course, is e^+e^- Bhabha scattering.

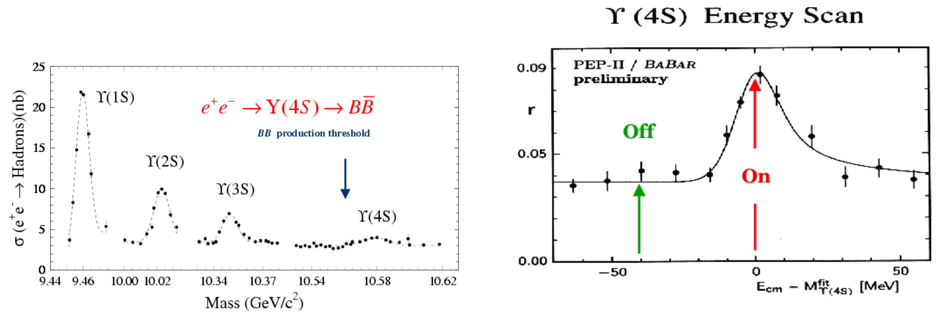

Figure 2.7: Left: Plot of the Υ resonances as a function of the e^+e^- center of mass energy. The $\Upsilon(4S)$ is right above the threshold for $\overline{b}$ quark production, and is a short-lived bound-state resonance. Right: Closeup of the $\Upsilon(4S)$ peak where the radiative tail is clear. The two arrows mark the E_{cm} energies where we collect collision data, “on” and “off” the resonant peak.

An ideal production mechanism for $B\overline{B}$ pairs is to create $\Upsilon(4S)$ particles and study their decay products which are essentially exclusively B (see Fig. 2.8). However, the energy release in the $\Upsilon(4S)$ decay is so small that the B decay products are nearly at rest in $\Upsilon(4S)$ frame. In short, the b quark mass is $m_b = 5.28\,\text{GeV}$, which is almost exactly half the mass of the $\Upsilon(4S)$ resonance leaving little extra for kinetic energy. This makes the observer’s job difficult: the B mesons don’t travel very far in the lab since they have such little momentum; in this case, it becomes extremely difficult to separate the B production point and its decay point. The technique proposed by Pier Odonne [21] is to produce the $\Upsilon(4S)$ so that it is traveling at moderate velocity in the lab frame. [¶] If the boost of the $\Upsilon(4S)$ is chosen wisely, modern particle detectors can then resolve the B production and decay vertices.

As described in detail later, we collide electron and positrons together at the PEP-II facility at SLAC [‖]. The novelty of the PEP-II design is the asymmetric energies of the circulating beams: the electrons are accelerated to 9.0 GeV and the positrons to 3.1 GeV. The center-of-mass is therefore boosted in the lab, travelling in the direction of the e^- beam with a boost of $\gamma\beta \sim 0.55$. The center-of-mass energy is slightly more

---

[¶] The boost in the lab frame also provides a small time dilation, but it is only a 10% effect.

[‖] Stanford Linear Accelerator Center, Menlo Park, California, USA

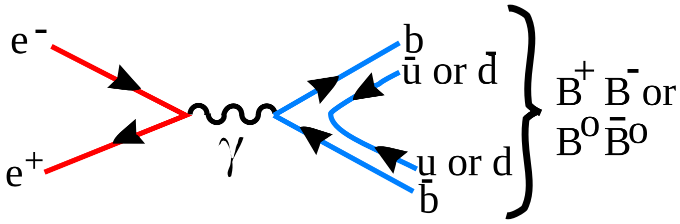

Figure 2.8: Feynman diagram for the $B\overline{B}$ production mechaniasm at the $\Upsilon(4S)$ resonance via a virtual photon.

than 10.5 GeV, near the production threshold of the $\Upsilon(4S)$ resonance. The $\Upsilon(4S)$ decay products (the $B\overline{B}$ pairs) "fly" in the lab, travelling hundreds of μm before their decay.

An additional benefit of working with the $\Upsilon(4S)$ decay is the correlated time evolution of the daughter B^0-$\overline{B}^0$ mesons. Akin to the EPR paradox with correlated photons, when the $\Upsilon(4S)$ decays and produces the B^0-$\overline{B}^0$ pair, we don't know which B is the $\overline{B}^0$ and which B the B^0; and because of their mixing, either can be either at any time. However, since the $\Upsilon(4S)$ is a vector, and the B mesons pseudoscalar bosons (*i.e.,* spin 0), we know that the B-$\overline{B}$ state must have $L = 1$ to conserve the angular momentum of the $\Upsilon(4S)$. This means that the B and $\overline{B}$ are in antisymmetric p-wave state. Because of mixing between the neutral B mesons, we might expect to occasionally have B^0-B^0 or $\overline{B}^0$-$\overline{B}^0$; this is forbidden however because that would leave us with identical bosons in an antisymmetric state, violating Bose statistics. We conclude therefore, that after the $\Upsilon(4S)$ decay, there can be at most one meson of each flavor.

2.3.2 Decays of the $\Upsilon(4S)$

We now have the ingredients for a time-dependent analysis. As shown in Fig. 2.9, the e^- and e^+ collide and form the resonant $\Upsilon(4S)$ state which immediately decays into a $B\overline{B}$ pair, either B^+B^- or $B^0\overline{B}^0$ (about half and half). If neutral, the pair time-evolves in a correlated fashion. At time t_1, one of the B's decays, which "starts the clock." At that exact instant, the surviving B must be of the opposite flavor,

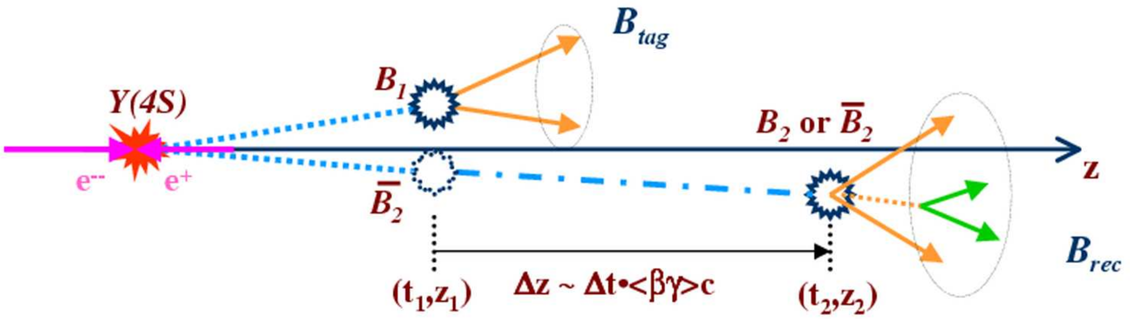

Figure 2.9: An artist's conception of the experiment. The $\Upsilon(4S)$ decays to two B mesons which later decay themselves. The decay products can be used to identify the vertex and flavor of each B at decay.

as explained above; it subsequently decays at some later time t_2. Because mixing is periodic and lifetime stochastic, the same physics governs B_2 between t_1 and t_2 as between its true origin (at the decay of the $\Upsilon(4S)$) and its final decay at t_2. We can use the decay products of each B to determine its decay vertex, and its flavor at decay. Because the B mesons are boosted in the lab frame along the z-axis, we can assume that most of their travel is along that axis (*i.e.,* the B mesons travel single file and along $\hat{z}$).

Our study of B^0 lifetime and mixing analyzes a large set of these $B\overline{B}$ pair events. We look for events in which we can exclusively reconstruct one B meson's decay in the semileptonic channel $B^0 \to D^{*-}\ell^+\overline{\nu}_\ell$ channel. [**] As in Fig. 2.9, the reconstructed B is denoted $B_{\rm rec}$, and we claim to understand it very well. The other B is called $B_{\rm tag}$, because it "tags" the flavor and location of our $B_{\rm rec}$ at the time t_1. To repeat: we know when and into what $B_{\rm rec}$ decayed because we have fully reconstructed it from its decay products; and we use the more inclusive information from $B_{\rm tag}$ to get "another data point" on the life-cycle (trajectory) of $B_{\rm rec}$. (Keep in mind that while the figure suggests that $B_{\rm rec}$ decays after $B_{\rm tag}$, this ordering is arbitrary – the argument still holds.)

[**] We imply charge conjugate modes wherever possible to reduce the notation, unless explicitly stated otherwise.

- We call a $B\overline{B}$ event *mixed* if $B_{\rm rec}$ has the opposite flavor at decay as it had at the tagging point. Consequently, $B_{\rm tag}$ will be measured as having the same flavor as $B_{\rm rec}$ at decay because it's the opposite of the opposite.

- Likewise, we call an event *unmixed* if $B_{\rm rec}$ is found to have the same flavor at decay and at the tagging point. (And so $B_{\rm tag}$ will be measured to have the opposite flavor.)

By measuring the separation in z between the two decay vertices, and using our knowledge of the boost in the lab frame, we can estimate Δt, the time between the two decays by using the relation:

$$\Delta t = \frac{\Delta z}{\langle \beta_z \gamma \rangle c} \tag{2.34}$$

This study accumulates measurements of mixing status (via flavor identification) and Δt for events with reconstructed $B^0 \to D^{*-}\ell^+\overline{\nu}_\ell$ decays, analyzes them to characterize and remove backgrounds (where possible), and then uses an unbinned maximum-likelihood fit to extract the time evolution parameters of the B^0 meson.

The $B_{\rm rec}$ is reconstructed in the decay chain, $B^0 \to D^{*-}\ell^+\overline{\nu}_\ell$, $D^{*-} \to \overline{D}{}^0\pi^-$, and $D^0 \to K^-\pi^+$, $K^-\pi^+\pi^0$, $K^-\pi^+\pi^-\pi^+$, or $K^0_S\pi^+\pi^-$ (summing to about 25% of the total D^0 branching fraction). Although the neutrino cannot be detected, the requirement of a reconstructed $D^{*-} \to \overline{D}{}^0\pi^-$ and an identified high-momentum lepton that satisfies the kinematic constraints consistent with a $B^0 \to D^{*-}\ell^+\overline{\nu}_\ell$ decay allows the isolation of a signal sample with (65 – 89)% purity, depending on the D^0 decay mode and whether the lepton candidate is an electron or a muon.

We reconstruct the D^* in the mode $D^{*-} \to \overline{D}{}^0\pi^-$, which has a branching fraction of 68%; because of the small mass difference, the momentum transfer is only 39 MeV. The emitted pion is therefore slow-moving in the D^* frame, and is often called the *soft* or *slow pion.* Due to the small energy release, accurate reconstruction of the soft pion is an experimental challenge.

2.3.3 Time Dependent Analysis

We are now ready to examine B^0-$\overline{B}^0$ time evolution as it might appear in *BABAR*. The strategy is to describe the Δt_{meas} distributions with a probability density function, build a full likelihood for the entire dataset, and then use an unbinned maximum likelihood fit to determine the parameters which best fit the data. Before describing the technique in subsequent chapters, we consider the realistic smearings and uncertainties that complicate that Δt distributions. In this study, we will model and parameterize these effects with coefficients extracted from the Data simultaneously with the physics parameters τ_{B^0} and Δm_d.

Based on the *mixed* and *unmixed* Δt distributions, we define the *mixing asymmetry* to be

$$A(\Delta t) = \frac{N_{\mathrm{unmixed}}(\Delta t) - N_{\mathrm{mixed}}(\Delta t)}{N_{\mathrm{unmixed}}(\Delta t) + N_{\mathrm{mixed}}(\Delta t)} , \tag{2.35}$$

The Δt_{true} distributions for events are shown in Fig 2.10. Note the complete absence of mixed events at $\Delta t_{\mathrm{true}} = 0$ because no time has elapsed for the B^0 to mix to $\overline{B}^0$. Also note that mixed distribution dominates in the intermediate range of Δt_{true}. Finally, the mixing asymmetry has unit amplitude and a period of $2\pi/\Delta m_d$.

The flavor identification algorithms at *BABAR* are not perfect, however, and we typically incorporate a *mistag rate* which parameterizes the rate at which we assign the $B^0\overline{B}^0$ event the wrong mixing status. (In the final analysis, we even allow the mistag rates for B^0 and $\overline{B}^0$ mesons to be different.) In this situation, we start trading events between the two curves in Δt_{meas} space, and we arrive at the distributions described in Fig. 2.11. Note that the mixing asymmetry amplitude has been *diluted* to $1 - 2\omega$ where ω is the mistag probability. Ideally, one could extract the mistag rate by measuring the amplitude of the mixing asymmetry at $\Delta t_{\mathrm{meas}} = 0$.

The final complication in imaging Δt_{true} in the experiment is due to finite resolution effects of the detector. Δt_{meas} will, in general, be a biased and smeared estimate of Δt_{true}, which can have dramatic effects on the measured Δt distributions as depicted in Fig. 2.11. To accommodate this, we include a resolution function in our model which maps the physics in Δt_{true} space into the real world of Δt_{meas}.

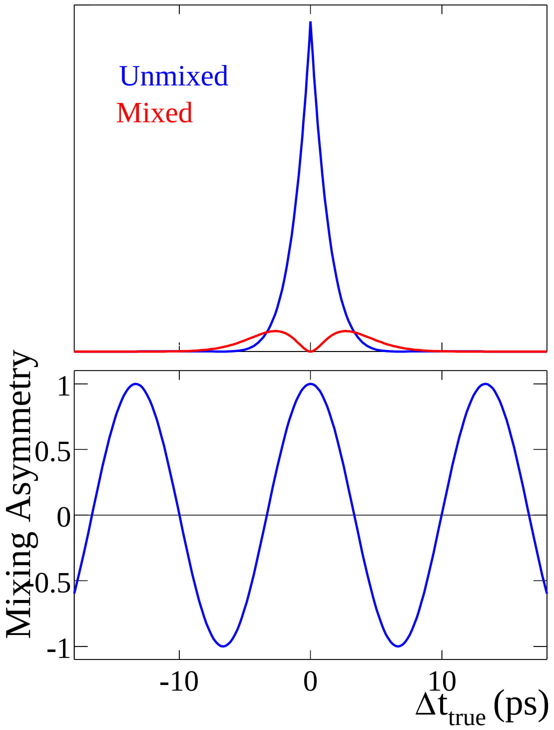

Figure 2.10: Upper: The distributions in $\Delta t_{\rm true}$ for mixed and unmixed $B^0\overline{B}^0$ events. Lower: The time dependent mixing asymmetry as defined in Eq. 2.35.

As we have suggested, the key principle in this time-dependent analysis is careful characterization of the Data while maximizing the statistical power of the event sample itself. That is, we try to minimize assumptions and external inputs in the analysis by adding components to the model (*i.e.,* mistag probabilities, background fractions, and resolution parameters) which will be determined simultaneously with the physics results in the final fit.

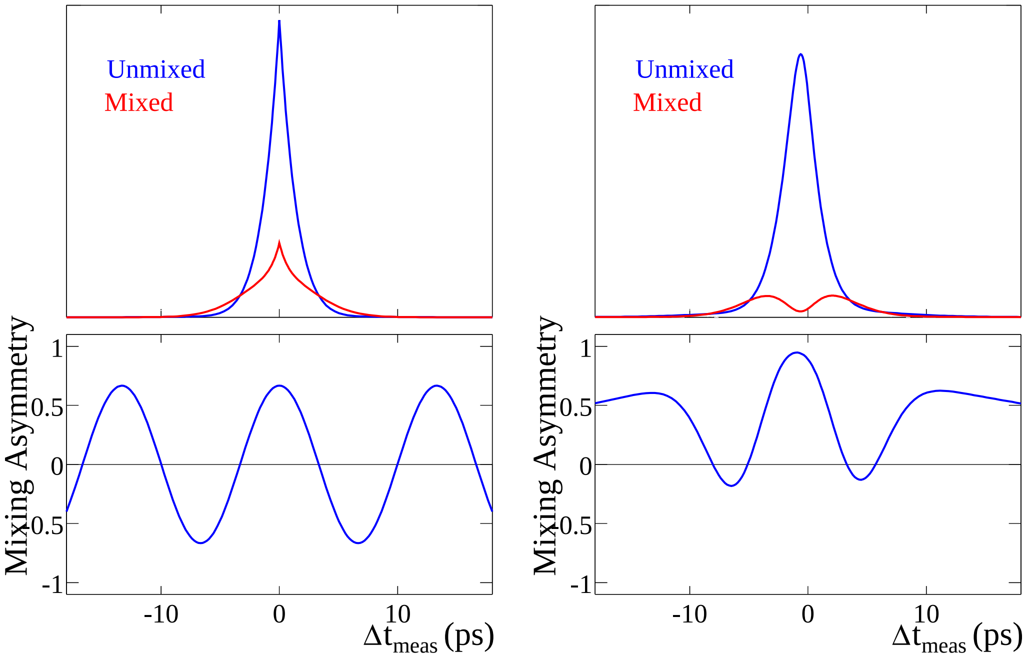

Figure 2.11: Upper Left: The distributions in Δt_{meas} for mixed and unmixed $B^0\overline{B}^0$ events with a mistag probability of 20%. Lower Left: The time dependent mixing asymmetry. Upper Right: The distributions in Δt_{meas} for mixed and unmixed $B^0\overline{B}^0$ events with an exaggerated resolution. Lower Right: The time dependent mixing asymmetry.

Chapter 3

Theory and Phenomenology

The framework for describing B meson time evolution is analogous to that of a 2-level system in quantum mechanics. Because the weak eigenstates are not identical to the physical eigenstates, a generic state has time-varying components of both B^0 and $\overline{B}^0$. The physical eigenstates have a mass splitting Δm_d and a lifetime difference $\Delta\Gamma$, where the latter is expected to be small in the Standard Model. Theoretical predictions for the mixing frequency Δm_d and the average lifetime τ_{B^0} still inherit significant uncertainties compared to the experimental precision.

The semileptonic decay mode $B^0 \rightarrow D^{*-}\ell^+\overline{\nu}_\ell$ is a three-body decay whose neutrino we do not reconstruct. We approximate the B center of mass frame as that of the $\Upsilon(4S)$, and construct angular variables which measure the consistency with the $D^{*-}\ell^+\nu_\ell$ decay.

3.1 Time Evolution Formalism

Neutral B mesons are produced in states of definite flavor, *i.e.,* flavor eigenstates. As suggested in Section 2.1.5, these states are not eigenstates of the weak interaction; we therefore expect the flavor to change under action of the electroweak Hamiltonian. We will first consider the form of an effective Hamiltonian to describe this process, find the new eigenstates and eigenvalues, and then consider their general time evolution.

3.1.1 Mixing of Neutral B Mesons

We borrow the formalism from that of a quantum mechanical two-level system where transitions are introduced by an interaction Hamiltonian, $\mathcal{H}$. The general state $|\Psi\rangle$ can be written as a linear combination of the flavor eigenstates, as they form a set of basis vectors in this subspace.

$$\begin{aligned} |B^0\rangle &= \begin{pmatrix} 1 \\ 0 \end{pmatrix} \qquad\qquad |\overline{B}^0\rangle = \begin{pmatrix} 0 \\ 1 \end{pmatrix} \\ |\Psi\rangle &= a|B^0\rangle + b|\overline{B}^0\rangle \\ &= \begin{pmatrix} a \\ b \end{pmatrix} \end{aligned} \tag{3.1}$$

We can decompose $\mathcal{H}$ in the flavor basis as:

$$\begin{aligned} \mathcal{H} &= \mathsf{M} - \frac{i}{2}\mathsf{\Gamma} \\ &= \begin{pmatrix} M_{11} & M_{12} \\ M_{21} & M_{22} \end{pmatrix} - \frac{i}{2}\begin{pmatrix} \Gamma_{11} & \Gamma_{12} \\ \Gamma_{21} & \Gamma_{22} \end{pmatrix} \end{aligned} \tag{3.2}$$

where M is the "dispersive" term representing virtual intermediate states and $\mathsf{\Gamma}$ is the "absorptive" term representing real intermediate states. Conservation of probability (*i.e.,* unitarity) requires $\mathcal{H}$ to be unitary, which forces M and $\mathsf{\Gamma}$ to be Hermitian matrices (the diagonal elements must be real, and the off-diagonal elements complex conjugates of each other, *e.g.,* $M_{12} = M_{21}^*$).

For the moment, we will also impose *CPT* symmetry, which requires that $M_{11} \equiv M_{22} = M$ and $\Gamma_{11} = \Gamma_{22} \equiv \Gamma$. Using the Wigner-Weisskopf approximation that the weak interaction Hamiltonian does not couple the final states to each other, [22] we write the time-independent Schrödinger equation, and wish to find the (energy) eigenvalues and eigenstates:

$$\begin{gathered} \mathcal{H}|\Psi\rangle = \lambda|\Psi\rangle \\ \begin{pmatrix} M - \frac{i}{2}\Gamma & M_{12} - \frac{i}{2}\Gamma_{12} \\ M_{12}^* - \frac{i}{2}\Gamma_{12}^* & M - \frac{i}{2}\Gamma \end{pmatrix} \begin{pmatrix} a \\ b \end{pmatrix} = \lambda \begin{pmatrix} a \\ b \end{pmatrix} \end{gathered} \tag{3.3}$$

where we assume $|\Psi\rangle$ is an energy eigenstate. Solving the equation $det[\mathsf{M} - \frac{i}{2}\mathsf{\Gamma} - \lambda] = 0$ yields a quadratic equation with two roots, the energy eigenvalues λ_+ and λ_-:

$$\lambda_\pm = M - \frac{i}{2}\Gamma \pm \sqrt{(M_{12} - \frac{i}{2}\Gamma_{12})\;(M_{12}^* - \frac{i}{2}\Gamma_{12}^*)}\;. \tag{3.4}$$

Substituting back in, we arrive at the rather cryptic forms for the new eigenstates:

$$|B_{1,2}\rangle = \left(\sqrt{(M_{12} - \frac{i}{2}\Gamma_{12})\;(M_{12}^* - \frac{i}{2}\Gamma_{12}^*)}\;|B^0\rangle \;\pm\; (M_{12}^* - \frac{i}{2}\Gamma_{12})\;|\overline{B}^0\rangle \right)\;, \tag{3.5}$$

where we have not included the normalization factors. By comparing the real and imaginary parts of the two eigenvalues, we realize that the two energy eigenstates have different masses ($m_{1,2} = \mathcal{R}e\ \lambda_\pm$) and different lifetimes ($\Gamma_{1,2} = -2\ \mathcal{I}m\ \lambda_\pm$); we associate the differences with the so-called *mass* and *(decay) width splittings*: [*]

$$\begin{aligned} \Delta m_d = m_1 - m_2 &= \mathcal{R}e\ (\lambda_+ - \lambda_-) \\ \Delta\Gamma = \Gamma_2 - \Gamma_1 &= 2\ \mathcal{I}m\ (\lambda_+ - \lambda_-)\;. \end{aligned} \tag{3.6}$$

---

[*] Note that we are using mixed notation here: τ_{B^0} for the B_d average lifetime, Δm_d for the mass splitting, and $\Delta\Gamma$ for the lifetime different. Apologies...the correctly labelled set of parameters should probably be Δm_d, $\Delta\Gamma_d$, and τ_{B_d}.

and deduce the following relationships

$$\begin{aligned}(\Delta m_d)^2 - \frac{1}{4}(\Delta\Gamma)^2 &= 4\ |M_{12}|^2 - |\Gamma_{12}|^2 \\ \Delta m_d\ \Delta\Gamma &= -4\ \mathcal{R}e\ (M_{12}^*\ \Gamma_{12})\ .\end{aligned} \tag{3.7}$$

Let us now update our notation so that we can easily discuss the new states, but still requiring *CPT* symmetry:

$$\begin{aligned}p &= \sqrt{(M_{12} - \frac{i}{2}\Gamma_{12})(M_{12}^* - \frac{i}{2}\Gamma_{12}^*)} \\ q &= M_{12}^* - \frac{i}{2}\Gamma_{12}^* \\ \frac{q}{p} &= \frac{\sqrt{M_{12}^* - \frac{i}{2}\Gamma_{12}^*}}{\sqrt{M_{12} - \frac{i}{2}\Gamma_{12}}} \\ \lambda_\pm &= (M - \frac{i}{2}\Gamma) \pm \frac{q}{p}\ (M_{12} - \frac{i}{2}\Gamma_{12})\ .\end{aligned} \tag{3.8}$$

This allows us to write the energy eigenstates as

$$\begin{aligned}|B_L\rangle &= p|B^0\rangle + q|\overline{B}^0\rangle \\ |B_H\rangle &= p|B^0\rangle - q|\overline{B}^0\rangle \\ \Delta m_d &= m_H - m_L = -2\mathcal{R}e\ (\frac{q}{p}(M_{12} - \frac{i}{2}\Gamma_{12})) \\ \Delta\Gamma &= \Gamma_L - \Gamma_H = -4\mathcal{I}m\ (\frac{q}{p}(M_{12} - \frac{i}{2}\Gamma_{12}))\ .\end{aligned} \tag{3.9}$$

(We use the convention that $CP|B^0\rangle = +|\overline{B}^0\rangle$ and that the real part of q/p is positive.) As an interesting sidenote, we introduce δ as the complex *CP*-violating parameter (in mixing):

$$\delta \equiv \langle B_L|B_H\rangle = |p|^2 - |q|^2 = \frac{-2\ \mathcal{I}m\ (M_{12}^*\Gamma_{12})}{(\Delta m_d)^2 + |\Gamma_{12}|^2}\ , \tag{3.10}$$

which measures the amount to which the energy eigenstates are equally composed of B^0 and $\overline{B}^0$. (We also note that in the presence of *CP* violation, then, the energy eigenstates are not orthogonal.) We can explicitly observe the effect of *CP*-violation in mixing as modifications to Δm_d and $\Delta\Gamma$:

$$\begin{aligned}(\Delta m_d)^2 &= \frac{4\ |M_{12}|^2 - \delta^2\ |\Gamma_{12}|^2}{1+\delta^2} \\ (\Delta\Gamma)^2 &= \frac{4\ |\Gamma_{12}|^2 - 16\ \delta^2\ |M_{12}|^2}{1+\delta^2}\ .\end{aligned} \tag{3.11}$$

In the limit of exact *CP* invariance ($\delta = 0$) the mass eigenstates coincide with the *CP* eigenstates, $CP|B_H\rangle = -|B_H\rangle$ and $CP|B_L\rangle = +|B_L\rangle$ and the mass difference and width difference are given by $\Delta m_d = 2|M_{12}|, \Delta\Gamma = 2|\Gamma_{12}|$. Thus, as stated earlier, the lifetime and mass differences of the physical eigenstates in B^0-$\overline{B}^0$ system can (and will) manifest themselves without *CP* violation.

3.1.2 Time Evolution of Neutral B Mesons

We now invoke the time-*dependent* Schrödinger equation to study the time evolution of the again-generic state $|\psi(t)\rangle$:

$$i\frac{\partial}{\partial t}\begin{pmatrix} a(t) \\ b(t) \end{pmatrix} = (\mathit{M} - \frac{i}{2}\mathit{\Gamma})\begin{pmatrix} a(t) \\ b(t) \end{pmatrix}\ . \tag{3.12}$$

The time-dependent generic state can just be written in terms of an admixture of the energy eigenstates with time-evolving amplitudes for each component (with appropriate choices for $a_{H,L}(0)$ to match the initial conditions):

$$\begin{aligned}|\psi(t)\rangle &= a_H(t)\ |B_H\rangle + a_L(t)\ |B_L\rangle \\ &= a_H(0)\ e^{-\lambda_+\ t}\ |B_H\rangle + a_L(0)\ e^{-\lambda_-\ t}\ |B_L\rangle\ .\end{aligned} \tag{3.13}$$

We can then substitute in the expressions for $|B_H\rangle$ and $|B_L\rangle$ in terms of the flavor eigenstates. We can construct a state $|B^0_{phys}(t)\rangle$ which is created at time $t = 0$ as purely B^0, and likewise for $\overline{B}^0$ as $|\overline{B}^0_{phys}(t)\rangle$. The general time evolution is summarized as:

$$\begin{aligned} |B^0_{phys}(t)\rangle &= f_+(t)\ |B^0\rangle + \frac{q}{p}\ f_-(t)\ |\overline{B}^0\rangle \\ |\overline{B}^0_{phys}(t)\rangle &= f_+(t)\ |\overline{B}^0\rangle + \frac{p}{q}\ f_-(t\ |B^0\rangle\ , \end{aligned} \tag{3.14}$$

where the notation $f_\pm$ is simply

$$f_\pm = \frac{e^{-i\lambda_+\ t} \pm e^{-i\lambda_-\ t}}{2} = \frac{1}{2} e^{(-im_1+\Gamma_1/2)\ t} \left[1 \pm e^{(-i\Delta m_d+\Delta\Gamma/2)\ t}\right]. \tag{3.15}$$

We can find the transition probability, or oscillation rate, for the physical states to oscillate from one flavor to the other by computing the projection of the $|B^0_{phys}\rangle$ onto the flavor eigenstates $|\langle B^0|B^0_{phys}\rangle|^2$ and $|\langle\overline{B}^0|B^0_{phys}\rangle|^2$. Using the fact that the flavor eigenstates are orthogonal, and after some algebra of complex numbers, [†] we arrive at

$$\begin{aligned} |\langle B^0|B^0_{phys}\rangle|^2 &= |\langle B^0|f_+|B^0\rangle + \langle B^0|\frac{q}{p}f_-|\overline{B}^0\rangle|^2 \\ &= |f_+|^2 = \frac{e^{-\Gamma t}}{2}\left[\cosh(\frac{\Delta\Gamma}{2}t) + \cos(\Delta m_d\ t)\right] \\ |\langle\overline{B}^0|B^0_{phys}\rangle|^2 &= |f_-|^2 = \frac{e^{-\Gamma t}}{2}\left[\cosh(\frac{\Delta\Gamma}{2}t) - \cos(\Delta m_d\ t)\right]\ , \end{aligned} \tag{3.16}$$

At time $t = 0$ there is zero probability for finding the *mixed* state, where the $|B^0_{phys}\rangle$ has oscillated into a $|\overline{B}^0\rangle$, but afterwards, the probability exhibits a cosine time dependence with a frequency governed by Δm_d. [‡] This time-dependent mixing probability directly expresses the fact that since the flavor eigenstates are not the eigenstates of the interaction Hamiltonian, a generic state's projection on the flavor-space basis vectors will in general evolve in time. This phenomenon is called *mixing.*

In the B^0 system, we note that $\Delta\Gamma \ll \Gamma$ because of the small number of final states accessible to both B^0 and $\overline{B}^0$ (see Section 2.1.5). Additionally, experimental measurements report that $x_d = \frac{\Delta m_d}{\Gamma} = 0.73 \pm 0.05$. [23] Together these suggest that

---

[†] Pardon this sentence construction, but we wouldn't want to suggest that algebra itself is *complex*!

[‡] Note that these probabilities are bounded in time because $\Delta\Gamma$ is, by definition, bounded by $2 \times \Gamma$.

$\Delta m_d \ll \Delta\Gamma$ so we can reasonably collapse the cosh term to unity. In the study described here, we will assume the $\Delta\Gamma = 0$, but please see Section 15.3.2 for some comments about relaxing this assumption.

3.1.3 Time Evolution From $\Upsilon(4S)$ Decays

One important lesson from quantum mechanics is that multi-particle systems must be treated collectively, in order to properly account for their potentially interfering amplitudes. The observer can really only make observations about the state of the system. At the $\Upsilon(4S)$, B mesons are produced in pairs, and they evolve coherently in an Einstein-Podolsky-Rosen correlated fashion; in particular, when they are neutral, they oscillate in phase. As such, then, we comment here on the so-called *coherent formalism* used to describe the time evolution of the $B\overline{B}$ system and its eventual decay to a set of final states $f_1,\ f_2$.

Following the description in Ref. [24], we write the general state containing two B mesons in the mass eigenstate basis as

$$|B\overline{B}\rangle = c_1|B_L B_H\rangle + c_2|B_H B_L\rangle \tag{3.17}$$

where $c_1,\ c_2$ are in general complex numbers satisfying the normalization condition $|c_1|^2 + |c_2|^2 = 1$. This state time-evolves just as the combination of the isolated states,

$$|B\overline{B}\rangle = |(B\overline{B})_{phys}(t_1,t_2)\rangle = c_1\, e^{-i\lambda_+ t_1} e^{-i\lambda_- t_2}|B_L B_H\rangle + c_2\, e^{-i\lambda_- t_1} e^{-i\lambda_+ t_2}|B_H B_L\rangle\ , \tag{3.18}$$

where $\lambda_\pm$ are the energy eigenvalues as before. We can use two arguments, as listed below, to derive constraints on the coefficients $c_1,\ c_2$.

Argument 1

The $\Upsilon(4S)$ is a vector meson, with $J = 1$, and $C \times P$ eigenvalue of $-1 \times -1 = +1$. Because the $\Upsilon(4S)$ decays via the strong interaction to the $B\overline{B}$ meson system, we expect CP to be conserved. Therefore, the daughter B B system's wavefunction must also have $CP = +1$. Consider the wavefunction as $\Psi_{flavor}\Psi_{space}$. The $B\overline{B}$ system must have one unit of orbital angular momentum, $L = 1$, since the B mesons are pseudoscalar bosons (*i.e.,* spin-0) and we need to conserve the angular momentum $J = L + S$ of the $\Upsilon(4S)$. The space part of the wavefunction Ψ_{space} is therefore negative under *CP*. To obtain an overall *CP* eigenvalue of +1, we are forced to choose the antisymmetric combination of the B and $\overline{B}$ to form the flavor part: $\Psi_{flavor} = |B\overline{B}\rangle - |\overline{B}B\rangle$ which also has $CP = -1$.

Argument 2

We can reach a similar conclusion by invoking Bose symmetry on the general $B\overline{B}$ mass eigenstate formalism. If both B mesons, in the $L = 1$ antisymmetric p-wave, were to decay simultaneously to identical bosonic final states f, then we would have two identical bosons in an antisymmetric state. This violates the requirements of Bose statistics. This has an immediate consequence for the coefficients $c_1,\ c_2$:

$$\begin{aligned}
|B\overline{B}\rangle &= c_1|B_L B_H\rangle + c_2|B_H B_L\rangle \\
\langle ff|B\overline{B}\rangle &= 0 \\
c_1\langle ff|B_L B_H\rangle + c_2\langle ff|B_H B_L\rangle &= 0 \\
c_1\langle ff|B_L B_H\rangle &= -c_2\langle ff|B_H B_L\rangle \\
\text{but} \quad \langle ff|B_L B_H\rangle &= \langle ff|B_H B_L\rangle \\
\therefore c_1 &= -c_2
\end{aligned} \tag{3.19}$$

Recall the normalization condition $|c_1|^2 + |c_2|^2 = 1$, so we see that up to an overall phase, we can set $c_1 = 1, c_2 = -1$. This conclusion that the two-meson state is antisymmetric in the mass eigenstate basis is equivalent to a statement about the system in the flavor eigenstate basis.

We therefore conclude that the $|B\overline{B}\rangle$ meson state is antisymmetric in flavor, which means that the projection on the set of states with two B^0 or two $\overline{B}^0$ mesons is vanishing; this is why we write the state as $|B\overline{B}\rangle$.

In the experimental program as outlined in Section 2.3.3, we noted that the time-evolution is recorded in terms of the variable Δt, the decay time difference, $\Delta t \equiv$

$t_2 - t_1$. We can change variables in Eq. 3.18 to achieve:

$$t \equiv \frac{t_1 + t_2}{2} \quad , \quad \Delta t \equiv t_2 - t_1 \tag{3.20}$$

$$|B\overline{B}(t, \Delta t)\rangle = e^{-i2\lambda t} \left\{ e^{+i\Delta\lambda\Delta t} |B_L B_H\rangle - e^{-i\Delta\lambda\Delta t} |B_H B_L\rangle \right\} \tag{3.21}$$

where we have introduced more notation,

$$\lambda \equiv \frac{\lambda_+ + \lambda_-}{2} = M - \frac{i}{2}\Gamma \quad , \quad \Delta\lambda \equiv \frac{\lambda_+ - \lambda_-}{2} = \frac{1}{2}\left(\Delta m_d - \frac{i}{2}\Delta\Gamma\right) \ . \tag{3.22}$$

We'll examine the case where one B decays to f_1 and the other to f_2 to make one observation which will complete our discussion. Taking the first B decay to f_1, we can write the *partially projected* state (borrowing again from Ref. [24]) as

$$\langle f_1 | B\overline{B}(t, \Delta t)\rangle = e^{-i2\lambda t} \left\{ e^{+i\Delta\lambda\Delta t} \langle f_1 | B_L\rangle \cdot |B_H\rangle - e^{-i\Delta\lambda\Delta t} \langle f_1 | B_H\rangle \cdot |B_L\rangle \right\} \ . \tag{3.23}$$

We next write the matrix elements in terms of the flavor eigenstates (the basis in which the physics of the actual decay is most easily described), introducing A_i as the quantum mechanical transition amplitude to a state i:

$$\begin{aligned} \langle f_1 | B_L\rangle &= p\langle f_1 | B^0\rangle + q\langle f_1 | \overline{B}^0\rangle = pA_1 + q\overline{A}_1 \\ \langle f_2 | B_H\rangle &= p\langle f_2 | B^0\rangle - q\langle f_2 | \overline{B}^0\rangle = pA_2 - q\overline{A}_2 \ . \end{aligned} \tag{3.24}$$

Combining this notation with that of the $|B^0_{phys}\rangle$, we can write the state after decay to f_1 at t_1:

$$\langle f_1 | B\overline{B}(t_1, \Delta t)\rangle = e^{-2i\lambda t_1} \left[|B^0_{phys}(\Delta t)\rangle \cdot \overline{A}_1 - |\overline{B}^0_{phys}(\Delta t)\rangle \cdot A_1 \right] \ . \tag{3.25}$$

The exponential factor out front is representative of the lifetime associated with the decay probability. If we choose the state f_1 to be accessible only to B^0, (*e.g.*, $B^0 \to D^{*-}\ell^+\overline{\nu}_\ell$), then we have $A_1 = 1, \overline{A}_1 = 0$, which identifies the decay as that of a B^0. (The state actually collapses to the time evolution for an isolated $\overline{B}^0$ meson after t_1.) If the other B decays to a state f_2 at time t_2, we can write the full decay amplitude as

$$\langle f_1 f_2 | B\overline{B}(t_1, \Delta t)\rangle = e^{-2i\lambda t_1}\left[\langle f_2 | B^0_{phys}(\Delta t)\rangle \cdot \overline{A}_1 - \langle f_2 | \overline{B}^0_{phys}(\Delta t)\rangle \cdot A_1\right] , \tag{3.26}$$

which we can use to compute the corresponding rate by taking the modulus-squared. Because of the B^0-$\overline{B}^0$ correlation, an interference term is introduced,

$$\begin{aligned} &\left|\langle f_1 f_2 | B\overline{B}(t_1, \Delta t)\rangle\right|^2 \propto \\ &\qquad e^{-2\Gamma t_1} \cdot \Big\{ \left|\langle f_2 | B^0_{phys}(\Delta t)\rangle\right|^2 \cdot \left|\overline{A}_1\right|^2 + \left|\langle f_2 | \overline{B}^0_{phys}(\Delta t)\rangle\right|^2 \cdot |A_1|^2 \\ &\qquad\qquad - 2\mathcal{R}e\ \left(\langle f_2 | B^0_{phys}(\Delta t)\rangle \langle f_2 | \overline{B}^0_{phys}(\Delta t)\rangle^* \cdot \overline{A}_1 A_1^*\right) \Big\} . \end{aligned} \tag{3.27}$$

The interference term is only non-zero for states f_2 to which both B^0 and $\overline{B}^0$ can couple, and is a direct consequence of the correlated time-evolution.

Finally, let us make a comment on the general structure of the decay rate when we substitute back in the Δm_d-$\Delta\Gamma$ form of the energy eigenvalues. The algebra is beyond the scope of this document, so we quote from Ref. [24]:

$$\begin{aligned} &\left|\langle f_1 f_2 | B\overline{B}(t, \Delta t)\rangle\right|^2 \propto \\ &\quad e^{-2\Gamma t}\left[c_1 \cosh(\frac{\Delta\Gamma\Delta t}{2}) + c_2 \cos(\Delta m_d \Delta t) + c_3 \sinh(\frac{\Delta\Gamma\Delta t}{2}) + c_4 \sin(\Delta m_d \Delta t)\right] , \end{aligned} \tag{3.28}$$

where the coefficients c_i obey a normalization condition and depend on the decay amplitudes A_1, A_2, their conjugates and the symmetries required of the theory. [§] If we assume $\Delta\Gamma \equiv 0$, the sinh term vanishes and the cosh term collapses to unity.

3.2 Comments on τ_{B^0}

One goal of this analysis is the measurement of τ_{B^0}, the average lifetime of the neutral B meson, often referenced as $1/\Gamma$. We comment here on some of the theoretical

---

[§] Note that (a) we can integrate out the t dependence at fixed Δt to achieve the overall decay time difference distribution and that (b) I have hidden some of the relationships between the c_i.

framework for Standard Model predictions of the lifetime.

Calculation of the average B lifetime can be estimated to first order through use of the *spectator model*, in which we assume the the lighter quark in the meson(here, the $\overline{d}$) is not involved in the decay dynamics. In fact, a spectator model would predict that the heavy b quark dictates the entire decay process, and in fact, would predict the B^+ and B^0 lifetimes to be identical, as governed by the primitive equation below. The B meson decay width is dominated by $b \rightarrow c$ (λ^2) transitions, bringing in V_{cb}, and $b \rightarrow u$ contributions are suppressed by V_{ub} (λ^3) which we can neglect: [25]

$$\Gamma = \frac{1}{\tau} \sim \frac{G_F^2 \; m_b^5}{192\pi^3} \cdot |V_{cb}|^2 \times \rho(E, \vec{k}) \; , \tag{3.29}$$

where $\rho(E, \vec{k})$ is the appropriate set of phase-space factors. Experiments have measured that $\tau_{B^+}/\tau_{B^0} = 1.062 \pm 0.029$ [26], which indicates a significant deviation from the naive expectations of the spectator model. This is understood to be due to complications such as W-exchange or weak annihilation and Pauli interference diagrams.

Applying the optical theorem, the inclusive decay width of a hadron H_b containing a b quark can be written as the forward matrix element of the imaginary part of the transition operator and a few Wilson coefficients which take into account QCD corrections. Since the energy release in the decay of b quark is relatively large, its possible to construct an Operator Product Expansion (OPE) for the decay rate. The forward matrix elements in the OPE are expanded in inverse powers of the b-quark mass, following the prescriptions of heavy-quark effective theory (HQET). [27] These calculations predict differences from unity in the lifetime ratio of up to 10%, consistent with the observed value. [¶] Measurement of the B lifetime can be an important test for models of spectator quark effects, and can be used to extract the semileptonic decay constant, f_{B_d}, discussed in the next section.

The lifetime τ_{B^0} is a critical input to the extraction of other parameters of the Standard Model, such as measuring V_{cb} using semi-leptonic decays. τ_{B^0} is also needed

---

[¶] The b quark is the heaviest quark with which we can test these heavy flavor models, as the top quark is so heavy it decays weakly before it even hadronizes.

in the study of *CP*-asymmetries since it is used to characterize the signal in time-dependent analyses.

3.3 Comments on Δm_d

Study of the mixing frequency Δm_d is motivated by two reasons:

- Measurements of Δm_d can be used to extract the CKM matrix element V_{td} and thus determine the length of one of the sides of the unitarity triangle.
- In principle, since neutral meson mixing involves loop contributions, Δm_d is sensitive to new physics because interactions at higher scales can produce changes in the local operators at lower scales.

The mixing frequency Δm_d corresponds to the off-diagonal element M_{12} of the Hamiltonian $\mathcal{H}$ which we discussed above, and is related to the dispersive part of the transition amplitude between B^0 and $\overline{B}^0$. [‖] The important corrections from QCD are implemented with the help of the operator product expansion. [5] The top-quark contribution dominates and we can describe M_{12} by the so-called "local $\Delta B = 2$" Hamiltonian below the electroweak symmetry breaking scale as [28]

$$\Delta m_d = \frac{G_F^2}{8\pi^2} M_W^2 \, |V_{td} V_{tb}^*|^2 \, \eta_B S_0(x_t) C_B(\mu) \, \frac{|\langle \overline{B}_d | \mathcal{O}_d^{\Delta B=2}(\mu) | B_d \rangle|}{2 M_{B_d}} \, , \tag{3.30}$$

where $x_t = m_t^2/M_W^2$, $S_0(x_t) \simeq 0.784\, x_t^{0.76}$ (to better than 1%) is the relevant Inami-Lim function [29], μ the renormalization scale, $\mathcal{O}_d^{\Delta B=2}$ the four-quark operator, [**] and $\eta_B = 0.55$ and $C_B(\mu)$ are short-distance coefficients. The renormalization-scale dependence of $C_B(\mu)$ and the hadronic matrix element cancel at the level of perturbative analysis. Typically, we are after $|V_{td} V_{tb}^*|^2$, and calculate $S_0(x_t)$, η_B and b_B perturbatively. Because V_{tb} is known to be close to unity to good accuracy, Eq. 3.30 enables extraction of V_{td}. The precision is limited at present by the precision of lattice

---

[‖] Ironically, although M_{12} is the real part of the amplitude from the box diagram, it describes virtual transitions.

[**] $\left[\overline{b}\gamma^\mu(1-\gamma^5)d\right] \; \left[\overline{b}\gamma_\mu(1-\gamma^5)d\right]$

QCD efforts to compute the hadronic matrix element. That matrix element is often parameterized as

$$\langle \overline{B}_d | \mathcal{O}_q^{\Delta B=2}(\mu) | B_d \rangle = \frac{8}{3} M_{B_d}^2 f_{B_d}^2 B_{B_d}(\mu) \; , \tag{3.31}$$

where f_{B_d} is the meson decay constant and B_{B_d} the so-called bag parameter. This matrix element is the subject of much debate, as different theoretical estimates using lattice QCD techniques give different results, although all agree that $f_{B_d}\sqrt{B_{B_d}} \sim 200\,\mathrm{MeV}$. It becomes easier to consider the ratio of mixing frequencies for B_d and B_s in which many of the uncertainties cancel ††:

$$\frac{\delta m_s}{\Delta m_d} = \frac{m_{B_s}}{m_{B_d}} \zeta^2 \left| \frac{V_{ts}}{V_{td}} \right| \; , \tag{3.32}$$

where $\zeta = (f_{B_d}\sqrt{B_{B_d}})\ ((f_{B_s}\sqrt{B_{B_s}}) \sim 1$ as estimated from lattice QCD at the level of 5-6%, significantly reducing the hadronic uncertainties. [26] It is in this direction that current efforts are focused. However, Δm_s hasn't been measured experimentally yet, so the utility of this technique is still limited.

The phenomenological and theoretical interest in Δm_d is high, and when combined with expected results in the B_s system, offers a significant battery of tests for the Standard Model.

3.4 The Decay $B^0 \rightarrow D^{*-}\ell^+\overline{\nu}_\ell$

As suggested earlier, we need to unmistakably reconstruct a B candidate in the event to make it useful. Ideally, we would make a list of techniques and algorithms and use them to process every event, maximizing our chances of reconstructing every possible B-decay mode known today. This would certainly be the most efficient way to find B_{rec} candidates, but as Wm. McDonough has observed, "We must seek to be effective, not just highly efficient." [30] By maximizing our efficiency, we inevitably sacrifice our purity; that is, we include candidates in our sample that are not true B decays. It becomes difficult to understand the backgrounds (mistakes) in our sample

---

[††] Assuming unitarity, of course

when we strive to include as much signal as possible.

It is for these reasons that our analysis focuses on one set of $B_{\rm rec}$ decay modes. We look for semileptonic decays of the B, which are distinguished experimentally by a high momentum lepton and a missing neutrino: $B^0 \rightarrow D^{*-}\ell^+\overline{\nu}_\ell$. The branching fraction for this decay channel is relatively high, about 4.6% [5]. This means that for every 100 decays of the B, about 5 of them will involve a D^* and an e, and another about 5 will yield a D^* and a μ. We discard all other events with other types of B^0 decay. However, the semileptonic features of the decay allow the collection of a sample with high efficiency and purity, as this decay has the largest branching fraction of any other exclusive B decay mode.

We define the *signal* for this analysis to be events in which at least one B decays into a final state:

- which contains a $D^{*\pm}$ and either an electron or a muon of the opposite charge produced by $W^\pm$ decay,
- where the D^* and ℓ originate from a common vertex, within the detector resolution,
- and which has the same time-dependent decay structure as the mode $B^0 \rightarrow D^{*-}\ell^+\overline{\nu}_\ell$.

Under this definition, the D^* and ℓ must either be direct decay products of a parent B^0 via $B^0 \rightarrow D^{*-}\ell^+\overline{\nu}_\ell$, or else be secondary decay products of short-lived resonances. The known resonances which we expect could contribute are radially and orbitally excited D states, [31] $Y_c = D_1^+, D_1'^+, D_2^{*+}$:

$$B^0 \rightarrow Y_c\, e^+e^-\ (X) \quad , \quad Y_c \rightarrow D^{*+}\ X'\ .$$

By requiring the D^* and lepton to originate from a common vertex within the detector resolution, we exclude leptons from intermediate τ or D^0 resonances. We require the lepton to be produced by $W^\pm$ decay, which excludes short-lived electromagnetic decays, such as $B^0 \rightarrow D^{*-}\omega\pi^+, \omega \rightarrow \pi^0 e^- e^+$.

Due to imperfections in our event selection, we also select some $D^*\ell\nu$ decays which have charged B parents, via the reaction:

$$B^\pm \to D^{*0}\ell^\pm\nu_\ell X.$$

These decays, due to detector resolution, can appear consistent with the signal B^0 decay kinematics and can thus contaminate our sample. We remedy this situation in the final analysis by incorporating their expected Δt structure into the model and explicitly measuring the contamination fraction.

The $D^{*-}\ell^+\nu_\ell$ decay is a three-body decay which means that the angular structure of the decay products is not uniquely specified by the kinematics. The variables $\hat{E}_\ell$ (the lepton energy in the B center of mass frame) and $\hat{Q}^2$ (the $W^\pm$ invariant mass equal to $m_X^2 - 2m_{B^0}\hat{E}_{D^*}$, where $\hat{E}_{D^*}$ is the hadron energy in the B frame) parameterize the phase space of the decay

$$d\Phi\left(B^0 \to D^{*-}\ell^+\nu_\ell\right) \propto d\hat{E}_\ell\, d\hat{Q}^2 \ ,$$

and so are useful for disentangling the effects of phase space and dynamics. Fig. 3.1 compares the distribution of decays in the plane of these two variables [‡‡] for three-body phase space and $B^0 \to D^{*-}\ell^+\overline{\nu}_\ell$ decays.

The variables $\hat{p}_{D^*}$ (magnitude of the hadronic momentum in the B frame) and $\cos\hat{\theta}_{D^*,\ell}$ (angle between the directions of the lepton and the D^* in the B frame) are completely correlated with the Dalitz variables $\hat{Q}^2$ and $\hat{E}_{\mathcal{L}}$:

$$\begin{aligned} \hat{p}_X &= \frac{1}{2m_B}\sqrt{\left(m_B^2 - (\hat{Q} + m_{D^*})^2\right)\left(m_B^2 - (\hat{Q} - m_{D^*})^2\right)} \\ \cos\hat{\theta}_{D^*,\ell} &= \frac{\hat{Q}^2 + m_\ell^2 - \hat{E}_\ell(m_B^2 + m_{D^*}^2 - \hat{Q}^2)/m_B}{2\hat{p}_{D^*}\hat{p}_\ell} \ . \end{aligned}$$

Because they are also not independent, cuts applied to more than two of these four variables are not independent ($\hat{Q}^2$, $\hat{E}_\ell$, $\hat{p}_{D^*}$, $\cos\hat{\theta}_{D^*,\ell}$). Figure 3.2 shows the distribution of these variables. Figure 3.2(a) shows that the hadronic momentum has a sharp

---

[‡‡] Yes, a Dalitz plot!

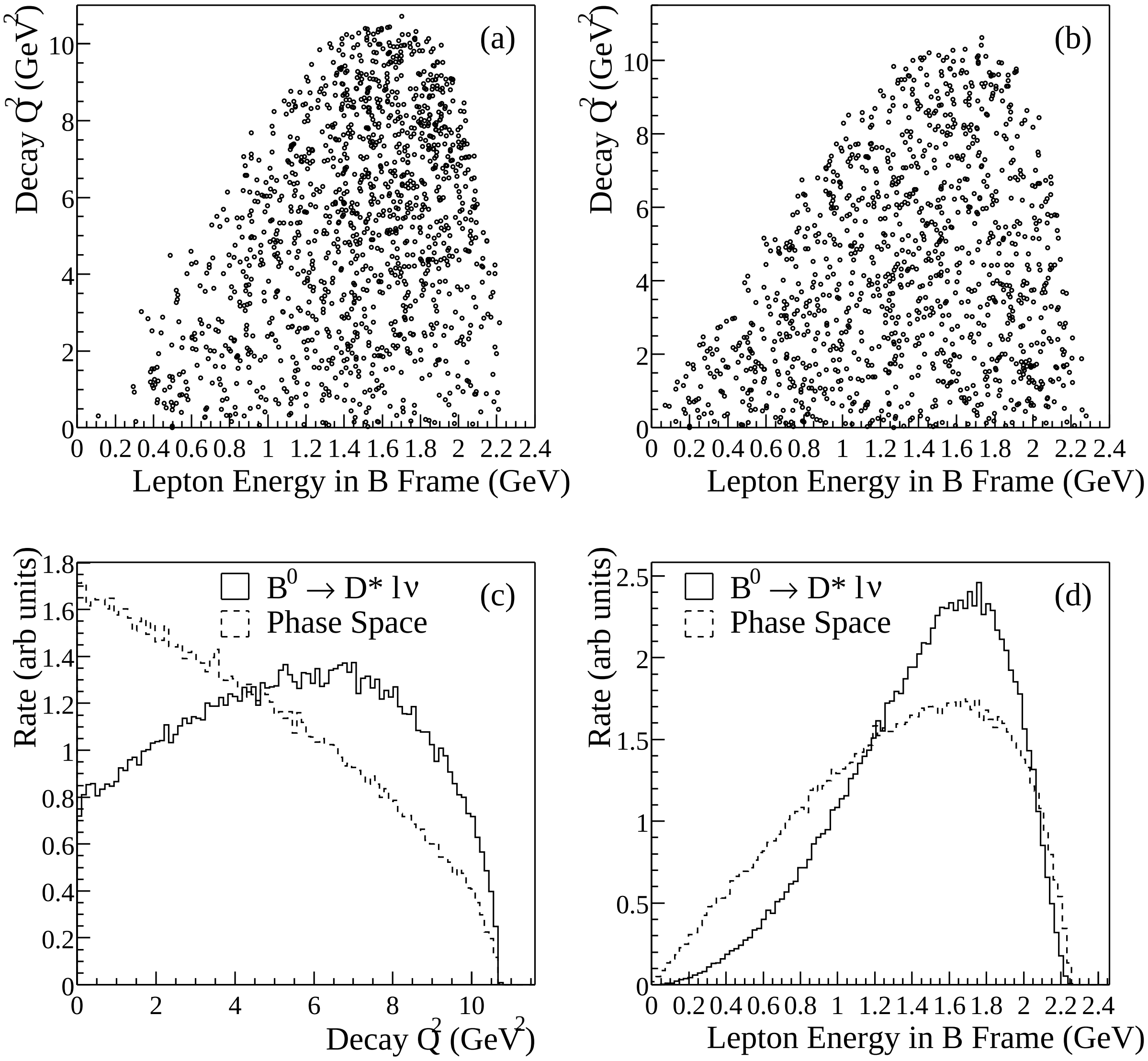

Figure 3.1: Dalitz distribution of $B^0 \to D^{*-}\ell^+\nu_\ell$ using (a) the form factors and angular-momentum correlations, or (b) three-body phase space. The lower plots show the normalized projections of these variables: (c) $\hat{Q}^2$, and (d) $\hat{E}_{\mathcal{L}}$.

edge at the upper kinematic limit, although the spectrum is significantly softened by the form factors and angular-momentum constraints (because of the $V - A$ structure of the weak interaction). Figure 3.2(b) shows that the D^* and lepton tend to be back-to-back in the B^0 decay frame, and that this effect is mostly due to phase space considerations.

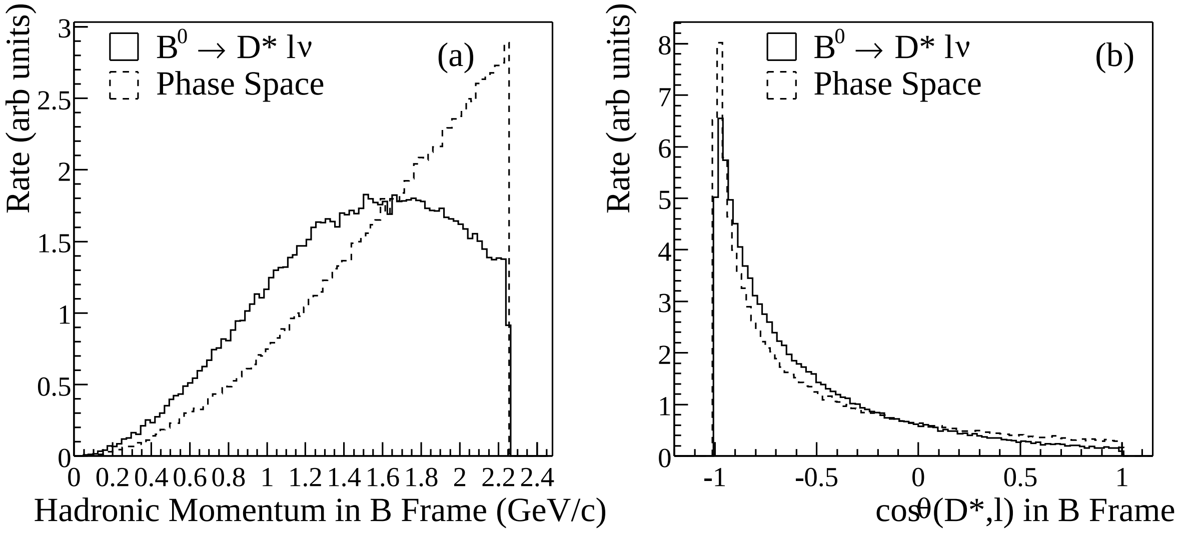

Figure 3.2: Normalized distributions of (a) the hadronic momentum, $\hat{p}_{D^*}$, and (b) the angle between the hadronic and lepton momenta, $\cos\hat{\theta}_{D^*,\ell}$, measured in the B^0 decay frame. The plots compare the distributions calculated using either three-body phase space, or else including the full decay dynamics.

Reconstruction of exclusive semileptonic decays is often more difficult than those which terminate in hadronic final states because of the undetected neutrino. Because of that deficit, there is no quantitative prescription for combining reconstructed D^* candidates with a lepton candidate to form a signal $D^*\ell$. (That is, we cannot build a B candidate because we don't have the daughter neutrino with which to apply the usual kinematic constraints.) At the $\Upsilon(4S)$, however, we can constrain the energy of the $B_{D^*\ell}$ candidate because we know the beam energy to high precision, so that $E_B = E_{beam}$. By comparing the sum of the four-vectors of the D^* and ℓ candidates with this constraint, one can test for consistency of the reconstructed D^* and ℓ system with a single missing neutrino (assumed to be massless). We can examine the missing invariant mass:

$$\begin{aligned} p_{D^*\ell} &= p_D^* + p_\ell \\ p_{miss}^2 &= p_\nu^2 = (p_B - p_{D^*\ell})^2 \\ &= m_B^2 + m_{D^*\ell}^2 - 2E_B E_{D^*\ell} + 2|\mathbf{p}_B||\mathbf{p}_{D^*\ell}| \cos\theta_{B,D^*\ell} \; . \end{aligned} \tag{3.33}$$

If the kinematics of the measured D^* and ℓ are really consistent with a missing neutrino, we expect the missing mass as expressed above to vanish. While this quantity is a Lorentz invariant, we note that it depends on p_B (magnitude and relative direction with respect to the $D^*\ell$) which, because of our lack of complete knowledge of the final state, is unknown. At the $\Upsilon(4S)$, $|\mathbf{p_B}| = 330\,\mathrm{MeV}$ which suggests that we could simply neglect the third term in the equation, effectively smearing the p_{miss}^2 distribution by the magnitude of the cross-term (about $0.5\,\mathrm{GeV}^2$). Another option is to assume the hypothesis is correct by setting $p_{miss}^2 = 0$, isolating the angular cross-term, and requiring that $\cos\theta_{B,D^*\ell}$ be in the physical range -1 to $+1$ to preferentially select candidates consistent with the hypothesis. This is the approach we use in this study.

Finally, we note that since the B momentum in the $\Upsilon(4S)$ frame is small, the two rest-frames are nearly co-moving. Assuming we know the beam energy and momentum very well, we often replace quantities in the B rest frame with quantities measured in the $\Upsilon(4S)$ frame because of the improved precision (and knowledge) in the $\Upsilon(4S)$ rest frame.

Chapter 4

Other Measurement Techniques

The study of the B meson lifetime and mixing frequnecy is not new; it's been a business for about two decades now. Dozens of other measurements of the B^0 lifetime τ_{B^0} and the mixing frequency Δm_d have been made. The large variety of techniques extract the same physics, but they differ in the strategies used to (a) produce and identify candidate B decays, (b) measure the flight length of the B, and (c) as needed for mixing, identify the b quark flavor. Additionally, most previous efforts have concentrated on measuring only one aspect of the time evolution. Time-dependent analyses, which use measurements of the decay time of each B candidate, have emerged as the preferred method for achieving high precision results.

4.1 Overview

In approaching the general task of studying B meson time dependence, it is important to understand the restrictions imposed by the "production" method: B physics can be studied at e^+e^- or hadron-hadron colliders, at threshold for B production or far above it. The three major groupings are

- hadron-hadron collisions: Experiments such as CDF and D0 [*] at the Tevatron rely on this mechanism in which protons and anti-protons are collided to produce $b\overline{b}$ quark pairs form parton-parton interactions. Hadronization yields uncorrelated B mesons, typically at high momentum and surrounded by a jet of other hadrons.

- e^+e^- interactions at the Z^0 pole or some other "higher" energy (30 – 90 GeV): Experiments at LEP, SLC, and PEP used this technique to create $b\overline{b}$ quark pairs from virtual Z^0 or γ interactions. The resulting B mesons are, again, heavily boosted in the lab frame, but the production vertex is known with good accuracy because of the small beamspot. However, the B mesons are still typically embedded in hadronic jets.

- e^+e^- interaction at threshold, the $\Upsilon(4S)$: As described earlier, the $\Upsilon(4S)$ resonance is just above the kinematic threshold for $b\overline{b}$ quark pair production, which provides a correlated pair of B mesons nearly at rest in the center-of-mass system. The subsequent decay of the B meson is relatively isolated, and "clean." CLEO uses this mechanism. The B production point is less well-known, however. A variation on this technique is the asymmetric B factory, which boosts the center-of-mass system in the lab frame. Both *BABAR* and Belle employ the asymmetric technique at the $\Upsilon(4S)$ resonance.

---

[*] And UA1

4.2 Lifetime

The general strategy for measuring particle lifetimes is to produce the particle directly and then reconstruct its decay length and momentum to extract the decay time. The decay time distribution is described with a negative exponential (lifetime) distribution, often convolved with some smearing or resolution function, usually Gaussian in nature. The analysis relies on correctly identifying events that contain B mesons, and cleanly measuring the production and decay points. One then needs an accurate model for converting measured flight distances to decay times — a momentum distribution resolution model. As such, lifetime measurements are inherently time-dependent analyses. Typically, the B meson system is boosted in the lab frame, increasing the flight path enough for imaging by precision tracking detectors. (This is the main reason that CLEO does not have a B lifetime measurement; the B decay vertex is too close to the production point for separation and distinction. They have, however, made some contributions by extracting the lifetime ratio from measurements of the B^+ to B^0 semileptonic branching ratios. [32])

The first measurements of the B^0 lifetime were reported in 1983 by the collaborations MAC [33] and MARK II [34] at the PEP facility. Their technique took advantage of the relatively large B semileptonic branching fraction by inclusively identifying b and c events with high momentum leptons from e^+e^- collisions at 30 GeV. The impact parameter of the lepton with respect to the interaction point was computed, and distribution was fit to find the average decay length of the B meson. Interestingly, the Mark II measurement included both leptons from charm and leptons from bottom as two separate samples in their analysis, and simultaneously estimated the c-quark meson and the b-quark meson lifetimes. [†] Note, however, that these measurements did not distinguish the type of B hadron produced, and so the results are actually average B hadron lifetime measurements. [‡]

[†] This use foreshadows the simultaneous technique using background control samples that is a key feature of this analysis.

[‡] At that time, B mesons were expected to have roughly identical lifetimes as dictated by the spectator quark model.

Measurements of τ_{B^0} have not changed significantly since these first efforts. Modern techniques use decay time measurements rather than projected impact parameters due to the advent of larger data samples that permit the "luxury" of exclusive reconstruction, and the development of silicon detectors for precise secondary vertex determination. Candidate reconstructions takes advantage of sophisticated particle identification technology to more efficiently select a purer sample of B decay candidates. Three different approaches are popular today, each having to do with how the B sample is collected, with tradeoffs between sample size and measurement precision.

- *Full Reconstruction:* Reconstructing the full decay chain of the B meson, typically using hadronic final states. This provides a good determination of the decay vertex and the boost, and incorporates little dependence on simulation. However, reconstruction efficiencies are low, typically 0.1%, so the statistical power is limited by small sample sizes. Both CDF and the asymmetric B-factories have capitalized on this technique.

- *Limited/Partial Reconstruction:* This approach uses the semileptonic decay mode of the B meson to identify candidates, either by identifying exclusive modes such as $B^0 \to D^{*-}\ell^+\overline{\nu}_\ell$ (but misses the neutrino), or by identifying the $D^{*-} \to \overline{D}^0\pi^-$ portion of the decay. This method is more efficient at B finding, and still allows for good decay vertex determination, but the incomplete knowledge of the event (even if only of just the neutrino) degrades the boost/momentum determination. There is a somewhat larger dependence on simulation, especially in the partially reconstructed case, where one needs to understand backgrounds in the selected sample. Almost every modern experiment has used this technique with some variations.

- *Inclusive Reconstruction:* The final approach is to inclusively identify B mesons, using minimal information about the details of the event. The cost of high signal efficiency is significantly larger backgrounds. At the B-factories, this is implemented as an inclusive dilepton analysis in which two high momentum leptons are used to identify candidate events and their distance of closest approach to the beamspot is used to estimate the decay length. At the higher $\sqrt{s}$

experiments, inclusive reconstruction can take advantage of *topological vertex reconstruction*, which Delphi has used with great success. Topological reconstruction of the vertex tries to assign all tracks in an identified b jet to either the primary or secondary vertex. The charge of the B is simply the sum of the charges of the tracks assigned to the secondary vertex. These methods (except at the B-factories where the higher mass B hadrons are not produced) suffer from contamination by B_s and Λ_B, however.

As of 2002, the most precise measurements come from the B-factories, closely followed by results from OPAL and SLD using the inclusive strategies. The industry of measuring τ_{B^0} will probably become secondary in the future, taking a back seat in the race to measure more sophisticated properties of B time evolution, *i.e.,* τ_{B^0} will be continue to be updated, but only as the byproduct of other analyses for which it is yet another floating parameter in the fit. However, if lattice QCD calculation converge on a precise prediction, interest in τ_{B^0} for its own sake might flare up.

4.3 Mixing Frequency

Strategies for measuring the neutral B mixing frequency come in two flavors [§], so-called "time-integrated" and "time-dependent" analyses. Time-integrated techniques seek to measure the mixing probability χ_d, where time-dependent analyses actually map out the oscillations of the B^0 mesons by recording the initial and final state flavor of the B^0 at the decay time. These techniques are used at all types of experiments,

The parameter χ_d is the integral of the $B^0 \to \overline{B}^0$ mixing probability (akin to Eq. 1.2), and if we assume *CP* invariance (and $\Delta\Gamma$ *equiv*0),:

$$\begin{aligned} \chi_d &\equiv \int \frac{\Gamma}{2} e^{-\Gamma t}(1 - \cos(\Delta m_d t)) \\ &= \frac{1}{2}\left[\frac{(\Delta m_d/\Gamma)^2}{1 + (\Delta m_d/\Gamma)^2}\right] \\ &= \frac{N_{mixed}}{N_{unmixed} + N_{mixed}} \end{aligned} \tag{4.1}$$

[§] Pun intended!

The time-integrated technique, then, relies only on detecting and accurately counting the number of mixed and unmixed B^0 events (assuming the efficiencies and misidentification probabilities for mixed and unmixed events are understood). With knowledge of the lifetime, one can immediately extract Δm_d. The earliest technique employed for identifying mixed and unmixed B^0 events uses the charge correlations of the lepton from B^0 semileptonic decays. The sign of the lepton's charge indicates the charge of the W, which in turn labels the flavor of the initial quark as b or $\overline{b}$. The key element counting the number of like-sign $B\overline{B}$ decays to measure the number of mixed events.

$B^0 - \overline{B}^0$ mixing was first reported in 1987 by ARGUS [1] (generally credited with the discovery) and UA1 [35]. ARGUS operated at the $\Upsilon(4S)$ resonance at the DORIS e^+e^- storage ring, and observed mixing in three different ways: by completely reconstructing one mixed event, by reconstructing B mesons in a set of hadronic and semileptonic final states and identifying the flavor of the recoiling B using a high momentum lepton, and by measuring the fraction of like-sign lepton $B\overline{B}$ decays. All three observations gave convincing evidence that B^0 was mixing into $\overline{B}^0$. CLEO has also reported precision measurements of χ_d, using similar time integrated techniques [36]. They expand upon the ARGUS technique by requiring only partial reconstruction of one B. The time-integrated technique is in principle the easiest, and perhaps most direct method, but it suffers from systematic uncertainties. Both CLEO and ARGUS ran at the $\Upsilon(4S)$ resonance where semileptonic decays of $B^{\pm}$, $c\overline{c}$, and $B^0\overline{B}^0$ daughters can dilute the sample. As of Summer 2002, the combined time-integrated measurement of the $B^0 - \overline{B}^0$ mixing frequency has an overall precision of 6.5%. [5]

The alternative to measuring the mixing probability is to observe the mixing dynamically, using a *time-dependent* analysis where better sensitivity is obtained. In this approach, the flavor of the candidate B meson is measured at two specific points in time. (Typically, this is the production and decay times. [¶]) The task reduces to the identification of signal B^0 candidates, *flavor-tagging* the initial and final states, and measuring the proper decay time. Flavor-tagging is the process of identifying the flavor of the b quark, often using charge correlations with the B decay daughters. Because most experiments produce $b\overline{b}$ pairs, such as $\Upsilon(4S) \rightarrow b\overline{b}$ or $Z^0 \rightarrow b\overline{b}$, the

---

[¶] But no at the B factories.

flavor of the B decaying on one side of the event is correlated with the flavor of the B on the other side. This is often used to provide the mixing status information. The proper time is estimated from the distance between the production point (usually the beamspot) and the B decay vertex (often relying on the precision tracking capabilities of silicon vertex detectors) and the B momentum. The decay time distributions are then used in a fit to extract the mixing frequency.

Different analyses employ different techniques to reconstruct the B meson whose decay time they measure. Exclusive reconstruction of final states is difficult in the higher energy experiments because of the multi-track jetty environments, so partial and inclusive reconstruction techniques have been preferred. An interesting note is that the LEP and Tevatron experiments use time evolution of uncorrelated B mesons; since the b and $\overline{b}$ quarks hadronize independently, one B meson can be charged and the other neutral. Different analyses also employ different techniques to measure the initial and final state flavors of the B. The algorithms can become quite elaborate, ranging from the use of high-momentum leptons, jet charge, reconstructed D^* charge, so-called charge dipole separation, and even the polar angle of the B candidate at SLD where the colliding beams were polarized.

The asymmetric B-factories follow this same time-dependent approach, but as described in Section 2.3.2, the decay time difference measurement is used, where the initial measurement of the B is not made at the production time, but rather at the time of the decay of the (correlated) other B. Time-dependent studies of B^0 mixing are typically limited by sample contamination, knowledge of the b-hadron lifetimes, and flavor-identification mistakes known as *mistags*. Before the B-factories, the world average on Δm_d using time-dependent techniques had an overall precision of about 2.6%, [5] significantly better than the time-integrated extractions discussed above.

4.4 Comparisons to This Measurement

As mentioned, this study is a time-dependent analysis, meaning that we directly observe the B meson's life-cycle. A novel feature of this study is the use of the asymmetric B Factory, which, by virtue of the asymmetric-energy head-on collisions, produces the B mesons at a moderate velocity along a single direction in the lab frame. The important advantage of this technique is that the B mesons travel a significantly longer distance in the lab (on average) before decaying, as compared to symmetric energy collisions at the $\Upsilon(4S)$. The decay distance difference becomes great enough to be resolved with modern particle detectors.

A key difference between the measurement reported here and those described above is the simultaneous extraction of Δm_d and τ_{B^0} using the same analysis on the same data sample. To date, there is only one other measurement of this (simultaneous) type in the B system, by OPAL at LEP, published in 2000 [37]. The OPAL result also uses the $B^0 \rightarrow D^{*-}\ell^+\overline{\nu}_\ell$ decay channel, where the Z^0 is approximated as a two-body decay: $Z^0 \rightarrow b\overline{b}$ and the D^0 decay is inclusively reconstructed amidst the b-jet. The proper time is reconstructed by measuring the energy of the B^0 and the decay length (separation of the e^+e^- beamspot and the combined lepton and π^-_{soft} tracks). They include energy resolution effects and a triple-Gaussian resolution function for the estimated proper decay time. The decay flavor of the B^0 candidate is determined by the sign of the lepton's charge, and the flavor at production is measured by studying the properties of the other b hadron. [‖] The event is divided into two hemispheres by a plane perpendicular to the thrust axis, one containing the candidate b jet, and the other opposite it. By considering the net charge of the other jet, reconstructed secondary vertices, and high momentum leptons in the the opposite hemisphere, an estimate of the other b flavor is made. The final fit uses the Δt distributions, resolution functions, $m(D^*) - m(D^0)$ spectra, and four different background models to simultaneously measure Δm_d and τ_{B^0} from a sample of about $80,000$ events with an overall precision better than 7% and 3% respectively. They also observe a statistical correlation between τ_{B^0} and Δm_d of -14%.

There are several reasons why we choose to fit the B^0 lifetime and oscillation frequency simultaneously. Traditionally, they have been studied separately, and the reasoning has been that (a) the lifetime is better measured without using the flavor identification information since biases and inefficiencies can be introduced by the

---

[‖] In the case where the other b hadronizes as a B^0, there will be some dilution due to its own mixing.

flavor-tagging algorithms, (b) at the true physics level, the lifetime and mixing parameters are completely uncorrelated, and (c) the world average value for the observable τ_{B^0} was typically far better than could be achieved in a single measurement. Our reasoning to the contrary is listed here:

1. The expected precision for both τ_{B^0} and Δm_d in this analysis is comparable to that of the year 2000 world average (an overall precision of 2% and 4%, respectively). Therefore, there is no benefit from fixating on the world average measurement of either. Depending on other measurements for parameter input (such as τ_{B^0}) introduces systematic uncertainties as well. The resolution on Δt leads to a correlation between τ_{B^0} and Δm_d. We can study the correlations between τ_{B^0} and Δm_d.

2. Mixing information improves the measurement of τ_{B^0} in two distinct ways:

   (a) Since mixed and unmixed events have different Δt distributions, the mixing information for each event gives greater sensitivity to the Δt resolution function and a smaller statistical uncertainty on τ_{B^0} by about 15%.

   (b) Since $B^0\overline{B}^0$ and B^+B^- events have different mixing behavior, we can use the Δt distributions for mixed and unmixed events to help discriminate between $B^0\overline{B}^0$ signal events and peaking B^+B^- background events.

3. The use of untagged events (actually, “poorly tagged events”) even for the mixing measurement increases our sensitivity to the resolution function. As will be described later, we use the tagging information from all events in the fit for lifetime and mixing.

4. Future measurements (see Chapter 15) which could extract $\Delta\Gamma$ and study the C, P, and T properties of B time evolution will need to re-evaluate the average values τ_{B^0} and Δm_d in the event that these additional parameters are found. (For instance, τ_{B^0} is measured assuming that $\Delta\Gamma$ is zero. If $\Delta\Gamma$ is nonzero (as expected), it will become more important as the precision of the τ_{B^0} measurement increases.)

Chapter 5

The BaBar Experiment

This study uses data collected with the BABAR detector at the PEP-II asymmetric-energy B-factory at SLAC, the Stanford Linear Accelerator Center in Menlo Park, California. The PEP-II accelerator collides 9.0 GeV *electrons and 3.1* GeV *positrons to produce $B\overline{B}$ pairs which decay quickly into sets of charged and neutral particles. These decay products in turn pass out of the beampipe collision volume into the BABAR detector, which consists of a series of concentric cylindrical detectors, each of which focuses on certain types of measurements. The momenta of charged particles are measured with a combination of a 40-layer drift chamber (DCH) and a five-layer silicon vertex tracker (SVT) in a 1.5-T solenoidal magnetic field. A detector of internally-reflected Cherenkov radiation (DIRC) is used for charged hadron identification. Kaons are identified with a neural network based on the likelihood ratios calculated from* $\mathrm{d}E/\mathrm{d}x$ *measurements in the SVT and DCH, and from the observed pattern of Cherenkov light in the DIRC. A finely-segmented CsI(Tl) electromagnetic calorimeter (EMC) is used to detect photons and neutral hadrons and to identify electrons. Electron candidates are required to have a ratio of EMC energy to track momentum, an EMC cluster shape, DCH* $\mathrm{d}E/\mathrm{d}x$*, and DIRC Cherenkov angle all consistent with the electron hypothesis. The instrumented flux return (IFR) contains resistive plate chambers for muon and neutral hadron identification. Muon candidates are required to have IFR hits located along the extrapolated DCH track, a suitable IFR penetration length, and an energy deposit in the EMC consistent with the muon hypothesis.*

The overarching goal of the *BABAR*-PEP-II facility is to study physics processes at the $\Upsilon(4S)$ resonance with high precision, including B, c, and τ physics. The primary focus is on decays of the neutral B meson, however. As suggested in Chapter 6,the B meson has a lifetime of only 1.5 ps, and at the $\Upsilon(4S)$ resonance, this corresponds to flight path in the lab too short to measure. By "boosting" the decay in the lab frame, we achieve better spatial separation of the decay and its products so that we can examine the physics more closely.

5.1 The PEP-II Facility

The PEP-II storage ring is the main engine of the experiment. PEP stands for *Positron Electron Project*, highlighting the fact that the system collides electrons and their antiparticles, positrons. The PEP-II facility is an upgraded version of the original PEP complex from around 1980. Both detector and accelerator personnel worked long and hard to bring all parts of the project online on-schedule and on-budget in May, 1999.

We list several important features of PEP-II here.

- PEP-II stores and maintains the energy of circulating 9.0 GeV electrons and 3.1 GeV positrons in two stacked storage rings. The asymmetric beam energies are necessary to produce center-of-mass collisions at the $\Upsilon(4S)$ resonance of 10.58 GeV, and boost the the $\Upsilon(4S)$ in the lab frame with $\beta\gamma = 0.55$. We refer to the higher-energy electron beam direction as the *forward* direction.

- The high beam currents and strong focusing of PEP-II are necessary to achieve the high luminosity required, in excess of $3 \times 10^33/\,\mathrm{cm}^2\,$ s. The PEP-II design was aggressive in its magnitude and scale, and it has performed above and beyond expectations. To provide final focusing as the beams come into collision, several accelerator components are actually inside the *BABAR* detector. The SLAC Linear Accelerator provides a high rate injector for the storage rings. Compared to other e^+e^- colliders, PEP-II has significantly higher beam currents due to the hundreds of so-called "bunches," the buckets of concentrated charge in the ring.

- The large data samples needed to achieve the physics goals of *BABAR* depend not only on the instantaneous luminosity of the accelerator, but also the *up-time*; that is, the fraction of each day that stable collisions are delivered. The *BABAR*-PEP-II team focuses on minimizing downtime in order to maximize the integrated luminosity.

Fig. 5.1 depicts the PEP-II rings and their relationship to the SLAC Linear Accelerator. For details of the PEP-II design parameters please see Ref. [38].

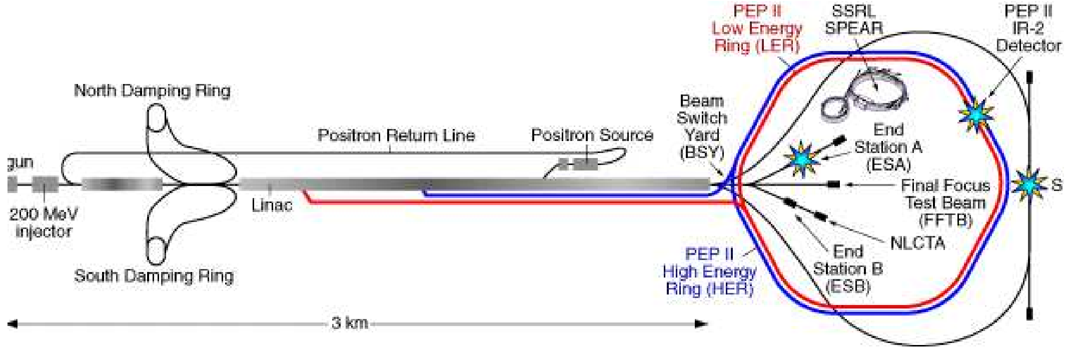

Figure 5.1: Schematic of the the PEP-II facility and SLAC. The 2 mile long Linear Accelerator provides intense beams of electrons and positrons which are injected into the PEP-II storage rings and come into collision at region IR-2.

The interaction region which includes the final focusing elements and the *BABAR* detector is a technical feat of modern engineering. We include an illustration of the final approach of the two beams in Fig. 5.2. The storage ring is, of course, not 100% efficient, as there are small losses around the ring where circulating charge is ejected from the nominal orbit. Primarily because of the high beam currents, these losses can sum to substantial radiation backgrounds in the *BABAR* detecotr, degrading not only instantaneous response (due to the presence of extra tracks, triggers, and noise) but also long-term performance through radiation damage. We refer the reader to the Appendices for several notes on these matters.

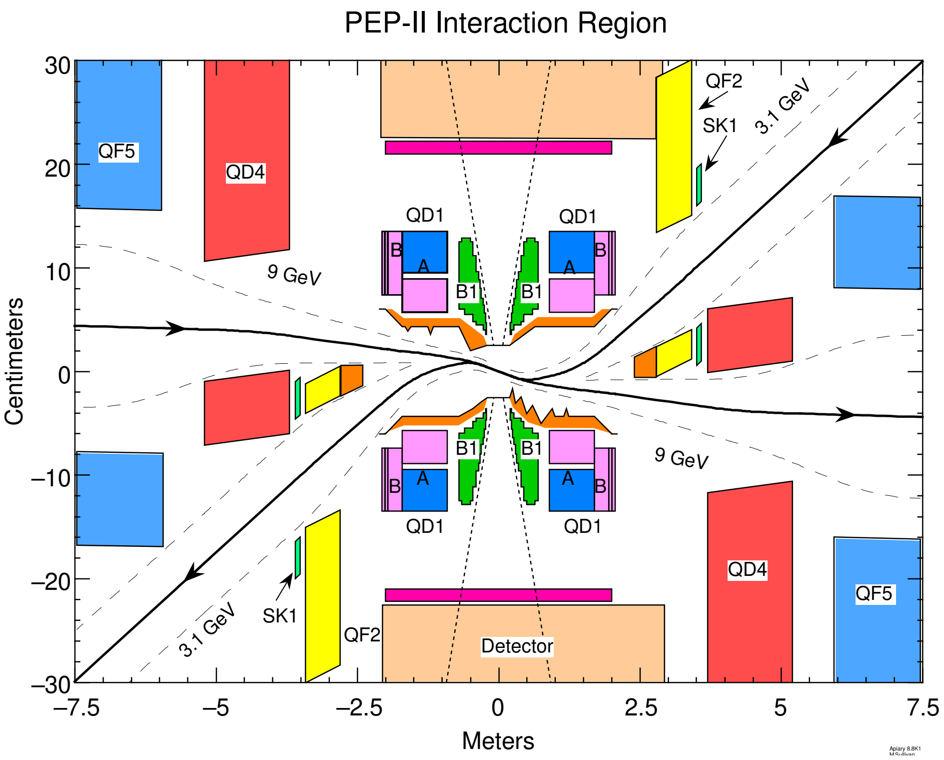

Figure 5.2: Plan view of the PEP-II interaction region, showing the focusing of the two beams in the magnetic elements. The beams collide head-on and are then separated. The strong focusing is achieved by the final doublets of quadropole magnets, Q1, Q2 and Q3, Q4. The internal B1 dipole magnets are permanent ferromagnets and perform the final bends to place the beams in (and out of) collision. (Diagram courtesy Ref. [39].)

5.2 The *BABAR* Detector

The *BABAR* detector is designed to quickly and accurately image the $B\overline{B}$ decay products as they travel outward from the interaction point. It is roughly a series of concentric cylinders surrounding the near-IR beamline. Fig. 5.3 shows a side- and end-view of the detector, illustrating its symmetries. In this Section, we'll touch upon each of the *sub-systems* of the detector, each of which consists of a separate cylindrical layer specialized in some functionality with specific types of instruments.